Accepted Manuscript

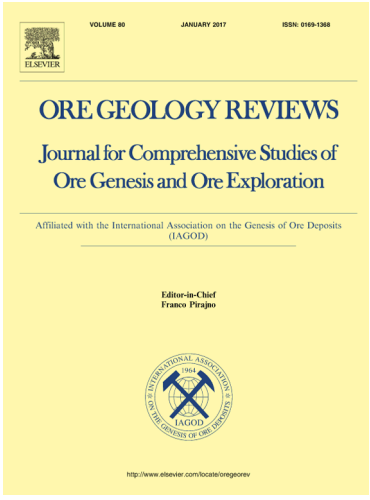

REE mineralogy and geochemistry of the Western Keivy peralkaline granite massif, Kola Peninsula, Russia

J.A. Mikhailova, Ya.A. Pakhomovsky, G.Yu. Ivanyuk, A.V. Bazai, V.N. Yakovenchuk, I.R. Elizarova, A.O. Kalashnikov

PII: S0169-1368(15)30184-0
DOI: http://dx.doi.org/10.1016/j.oregeorev.2016.11.006
Reference: OREGEO 2007

To appear in: *Ore Geology Reviews*

Received Date: 6 November 2015
Revised Date: 7 November 2016
Accepted Date: 10 November 2016

Please cite this article as: J.A. Mikhailova, Ya.A. Pakhomovsky, G.Yu. Ivanyuk, A.V. Bazai, V.N. Yakovenchuk, I.R. Elizarova, A.O. Kalashnikov, REE mineralogy and geochemistry of the Western Keivy peralkaline granite massif, Kola Peninsula, Russia, *Ore Geology Reviews* (2016), doi: http://dx.doi.org/10.1016/j.oregeorev.2016.11.006

REE mineralogy and geochemistry of the Western Keivy peralkaline granite massif, Kola Peninsula, Russia

J.A. Mikhailova, Ya.A. Pakhomovsky, G.Yu. Ivanyuk, A.V. Bazai, V.N. Yakovenchuk, I.R. Elizarova, A.O. Kalashnikov

Andrey O. Kalashnikov (kalashnikov@geoksc.apatity.ru, phone: +78155579628; **corresponding author**)

1) Geological Institute of the Kola Science Centre, Russian Academy of Sciences (GI KSC RAS). 184209, 14 Fersman Street, Apatity, Murmansk Region, Russia

Gregory Yu. Ivanyuk (ivanyuk@geoksc.apatity.ru),
Julia A. Mikhailova (ylya_korchak@mail.ru),
Yakov A. Pakhomovsky (pakhom@geoksc.apatity.ru),
Victor N. Yakovenchuk (yakovenchuk@geoksc.apatity.ru),
Ayya V. Bazai (bazai@geoksc.apatity.ru)

1) Geological Institute of the Kola Science Centre, Russian Academy of Sciences (GI KSC RAS). 184209, 14 Fersman Street, Apatity, Murmansk Region, Russia

2) Nanomaterials Research Centre of the Kola Science Centre, Russian Academy of Sciences. (NRC KSC RAS). 184209, 14 Fersman Street, Apatity, Murmansk Region, Russia

Irina R. Elizarova (elizarir@yandex.ru)

3) I.V. Tananaev Institute of Chemistry and Technology of Rare Elements and Mineral Raw Materials, Russian Academy of Sciences Kola Science Center (ICTREMRM KSC RAS). 184209, 26a Academic town, Apatity, Murmansk region, Russia.

Graphical abstract

Abstract

The authors have studied the geology, geochemistry, petrology and mineralogy of the rare earth elements (REE) occurring in the Western Keivy peralkaline granite massif (Kola Peninsula, NW Russia) aged 2674±6 Ma. The massif hosts Zr- and REE-rich areas with economic potential (e.g. the Yumperuaiv and Large Pedestal Zr-REE deposits), where 25% of ΣREE are represented by heavy REE (HREE). The main REE minerals are: chevkinite-(Ce), britholite-(Y) and products of their metamict decay, bastnäsite-(Ce), allanite-(Ce), fergusonite-(Y), monazite-(Ce), and others. The areas contain also significant quantities of zircon reaching potentially economic levels. We have discovered that behavior of REE and Zr is controlled by alkalinity of melt/solution, which, in turn, is controlled by crystallization of alkaline pyroxenes (predominantly aegirine) and amphiboles (predominantly arfvedsonite) at a late magmatic stage. Crystallization of mafic minerals leads to a sharp increase of K_2O content and decrease of SiO_2 content that cause a decrease of melt viscosity and REE and Zr solubility in the liquid. Therefore, REE and zirconium immediately precipitate as zircon and REE-minerals. There are numerous pod- and lens-like granitic pegmatites within the massif. Pegmatites in the REE-rich areas are also enriched in REE, but HREE prevails over light REE (LREE), about 88% of REE sum.

Keywords: REE geochemistry, REE mineralogy, peralkaline granite, Kola Alkaline Province

Highlights

- The Western Keivy massif hosts Zr-REE deposits with HREE representing about 25% of REE sum
- The main REE minerals are chevkinite-(Ce), bastnäsite-(Ce), fergusonite-(Y) etc.
- Alkali mafic minerals crystallization triggers REE minerals precipitation.
- There are numerous pegmatites with HREE mineralization.

Introduction

Alkaline complexes usually host high field straight elements (HFSE; Zr, Ti, Nb, Ta) and rare earth elements (REE) mineralization (Salvi and Williams-Jones, 2005). Recent advances in the industry aroused interest in these elements. This requires detailed studies of HFSE and REE concentration conditions. The most important heavy REE (Gd–Lu and Y) deposits are associated with peralkaline granites (e.g., Strange Lake, Canada; Miller, 1986) and their weathering crusts (e.g., deposits of Nanling Range, China; Ishihara et al., 2008).

Peralkaline granites with Zr-REE mineralization are well known at the Kola Peninsula (NW Russia). The mineralization have been studied since 1950s, when it was discovered that it is predominantly located within endocontact zones of granite massifs. In total, 2 deposit and 20 occurrences of REEs, Nb, Zr, U and Th were discovered here (Gaskelberg et al., 1978). However, in 1970-80s scientific and practical importance of these prospects decreased because the USSR's demand in LREE (La-Eu) was completely satisfied by the Lovozero REE-Ta-Nb deposit, and HREE were not widely used by the industry. Sharp growth of HREE demand in the 21st century and their strategic role in the military industry, on one hand; alongside with the Chinese monopoly and absence of explored deposits of these metals in Russia, on the other hand (Chakhmouradian et al., 2015), have caused another campaign of Zr-REE occurrences studies at the Western Keivy peralkaline granite massif. Total prospecting resources of REE_2O_3 within these occurrences are about 100 kt (Gaskelberg et al., 1978; Konopleva et al., 2012; Kalashnikov et al., 2016). It is not much in comparison with resources of the Khibiny and Lovozero massifs; however the REE occurrences in peralkaline granite are important due to high proportion of HREE in these rocks.

The main objective of our work is to define geochemical mechanisms of REE concentration.

Materials and methods

First of all, we have analyzed all available published and unpublished data on Zr-REE deposits and occurrences within the Western Keivy peralkaline granite massif (Porotova, 1959; Batieva, 1976; Gaskelberg et al., 1978; Chukhina et al., 1963; and others). At this stage, we have carried out our work 12 field traverses intersecting contacts of the massif (Fig. 1). During 2012-2013 field works, we took 89 samples along the traverses with lag 1–50 m, and documented about 20 pegmatite and pegmatite-like bodies. Alongside with sampling, we constantly measured radioactive background (with radiometer SRP-200) at 50 cm above the ground.

Major elements were determined by "wet" chemical analysis (GI KSC RAS), and REEs – by ICP-MS (PerkinElmer ELAN 9000 DRC-e, Institute of Chemistry and Technology of Rare

Elements and Mineral Raw Materials).

All minerals were identified with LEO-1450 scanning electron microscope equipped with Quantax EDS microanalyzer (BSE images, EDS analyses, cathodoluminescence analysis). Quantitative mineral composition was measured with MS-46 Cameca electron microprobe operating in WDS mode at 20 kV and 20–30 nA at the Geological Institute of the Kola Science Center (Russian Academy of Sciences). Beam diameter varied from 1 to 20 μm (depending on mineral stability). Standards and limits of accuracy applied for each element measurement are shown in Table 1. For statistical analysis, resulting values below the limit of accuracy were considered to be ten times lower than the limit.

Crystal-chemical formula calculations were carried out with the Minal program (software by D.V. Dolivo-Dobrovolsky, IGGD, Saint-Petersburg). Statistical analysis was carried out with STATISTICA 8 (StatSoft).

Geology and petrography of the Western Keivy peralkaline granite massif

The Keivy block forms a part of the Kola fold system in the north-eastern area of Fennoscandinavian Shield (Fig. 1A). It is a graben bounded by the North Kola deep fault in the north, and the Proterozoic Imandra–Varzuga greenstone belt. Metamorphic complexes of the Keivy block are divided into two structural stages. The lower one consists of garnet-biotite, muscovite-biotite, amphibole-biotite gneisses and amphibolites of Lebyazhinskaya series (AR_2), and the upper one is represented by the Keivy series (AR_2) consisting of kyanite, staurolite, garnet-sillimanite, carbonaceous schists and quartzites, as well as metamorphosed basic tuff-conglomerates and metavolcanics (Vetrin and Rodionov, 2009; Kozlov et al., 2006).

Peralkaline granites in the western part of the Keyvy block were discovered by B.M. Kupletsky and O.A. Vorobyova in 1928 (Kupletsky and Vorobyova, 1930). The area of the Western Keyvy peralkaline granite massif (sometimes called “Zapadnokeivsky massif”) is about 1300 km^2. Its age is 2674±6 Ma (Mitrofanov et al., 2000). The massif has a complex U-shape; however, its contacts with host metamorphic rocks are conformable (Fig. 1B). The contacts are usually sharp (Fig. 2), with aureoles of weak fenitization. There are many layer-like granite apophyses within host gneisses, as well as numerous xenoliths of gneiss within granite intrusion (Kharitonov, 1958; Batieva, 1976).

Rock-forming minerals of these peralkaline granites are quartz, albite, microcline, pyroxenes (aegirine, aegirine-augite), amphiboles (arfvedsonite, ferrorichterite, katophorite, riebeckite, ferroedenite) and aenigmatite. Typical accessory minerals include ilmenite, magnetite, titanite, pyrrhotite, zircon, fluorapatite and monazite-(Ce). Volume proportions of

felsic minerals are: 35 (± 5) vol. % of quartz, 30 (± 5) vol. % of microcline and 25 (± 5) vol. % of albite. Total content of mafic rock-forming and accessory minerals is about 10 (± 5) vol. %. In accordance with QAPF classification of igneous rocks (Le Maitre, 2002), all analyzed rocks were attributed to "alkali feldspar granite" field. Since the rocks always contain alkali clinopyroxenes and amphiboles, they should be termed "peralkaline granite".

The Keivy peralkaline granite is medium-grained (average grain size of rock-forming minerals is 1.2–2.7 mm) to fine-grained (average grain size of rock-forming minerals is 0.5–1 mm) rock. There is a gradual decrease of average grain size of this rock towards the contact with host gneisses (Fig. 2B, Fig. 3). Besides, the rock structure is gradually changing from massive in internal part of the massif to gneissose at the contact with host gneisses (Fig. 3): first, co-oriented lens-like segregations of dark-colored minerals appear in originally massive granite, then these minerals form bands alternating with the quartz-feldspar layers. Total content of mafic minerals in gneissose peralkaline granite (about 20 modal %) exceeds their content in massive granite (Fig. 3). Large near-contact zones of gneissose peralkaline granite are shown in Fig. 2B; however, small areas of this rock (from several meters to tens of meters) also occur sporadically in internal part of the massif.

Detailed petrographic study of peralkaline granites of the Western-Keivy massif has shown that quartz is an earlier magmatic mineral forming rounded or irregularly shaped grains (Fig. 4A, B, D). The next mineral is albite that occurs as irregularly shaped grains in interstices of quartz aggregate (Fig. 4A, D). A little later, microcline crystallized in the interstices of quartz-albite aggregate as xenomorphic grains that become well shaped at the contacts with dark-colored minerals (Fig. 4A, B). Mafic rock-forming silicates (aegirine-augite, aegirine, arfvedsonite, ferrorichterite, riebeckite, ferroedenite, katophorite, phlogopite and aenigmatite) crystallized after quartz and feldspars and occur as xenomorphic grains with indented boundaries and numerous poikilitic inclusions of earlier felsic minerals (Fig. 4A, B). Usually, clinopyroxenes and amphyboles are co-crystallized (Fig. 4 B); however, presence of poikilitic inclusions of aegirine in arfvedsonite grains and rims of this amphibole around aegirine-augite crystals (Fig. 4 C) indicate a later or/and longer amphibole formation. Aenigmatite occurs as euhedral or subhedral grains within amphibole crystals (including rims around clinopyroxene grains), i.e. it crystallized after clinopyroxenes and before amphiboles. Typical accessory minerals — ilmenite and magnetite — form small (up to 250 μm) inclusions in microcline, clinopyroxenes (Fig. 4A, B) and amphiboles as well as xenomorph grains in interstices between grains of rock-forming minerals. Accessory zircon occurs as small (up to 200 μm) inclusions in all rock-forming minerals, chains of rounded grains (up to 0.5 mm) along grain boundaries of rock-forming minerals and cracks in crystals of clinopyroxenes and amphiboles (Fig. 4A, B, D). This

association zircon+pyroxenes/amphiboles is the most common. In addition, zircon forms irregularly shaped segregations of small (up to 80 μm) short prismatic to isometric rounded grains in close intergrowths with magnetite.

Numerous accessory REE-bearing minerals occur in interstices of all abovementioned minerals, but they are irregularly distributed within the rock. Fluorapatite, titanite and monazite-(Ce) are found in 80–100 % of analyzed samples, and their content is rather constant. Fergusonite-(Y), allanite-(Ce), britholite-(Ce), chevkinite-(Ce), bastnesite-(Ce) and pyrochlore group minerals together with zircon and magnetite form rich disseminations in marginal parts of the peralkaline granite massif (0.2–3 km from the contact with host gneisses), and can be easily detected during field observations as radioactive anomalies (see Fig. 3). REE-rich zones extend along contacts with gneisses forming areas up to 1.5 x 4 km (the Yumperuaiv deposit; Fig. 1B). In these areas, total content of REE-rich minerals exceeds 5 vol. %, and several REE occurrences and deposits were discovered in the Western Keivy peralkaline granite massif in 50-70s of the 20th century: Yumperuaiv, Large Pedestal, Marya, Lebedinoe Lake, Belaya Golovka and others (Fig. 1B). The most important deposits are the Yumperuaiv and Large Pedestal deposits. Inferred resources of REE_2O_3 in Yumperuaiv deposit are 60 kt @ 0.55 wt. % (Chukhina et al. 1963; Gaskelberg et al., 1978). HREE represent about 1/3 of ΣREE. According to our estimation, inferred resources of REE_2O_3 in Large Pedestal deposit are 36 kt @ 0.33 wt. %. HREE represent about 1/4 of ΣREE. The deposits contain also significant quantities of zircon (up to 8 vol. %); and therefore, they can be regarded as Zr-REE deposits.

Petrographic features of peralkaline granite enriched in REE-bearing minerals (rock-forming minerals, sequence of their crystallization (Fig. 5), rock structure, grain size, etc.) are the same as the petrogtraphic features of surrounding granite with low content of such minerals (see Fig. 3). In this paper, for convenience, the first rock will be referred to as “REE-rich” granite, and the second — as “ordinary” granite.

There are numerous pod- and lens-like granitic pegmatites (average thickness 3 m, maximum — 20 m) within both REE-rich and ordinary granites. The largest pegmatites are found at Mt. Maly Pedestal, Mt. Rovgora and Mt. Ploskaya. Usually, the central zone of such pegmatite bodies (up to 5 m thick) consists mainly of quartz (90–95 vol. %) with inclusions of well-shaped green microcline (amazonite) crystals (up to 4 cm long) and graphite globules (up to 1 mm in diameter) (Fig. 6); the selvages (up to 5 m thick) formed by tabular to isometric microcline (amazonite) crystals (up to 60 cm in diameter); and the intermediate zone including tabular crystals of albite (up to 10 cm in diameter), short-prismatic crystals (up to 8 cm long) of Na-Ca and Na amphiboles (arfvedsonite, ferrorichterite and katophorite), aegirine and aegirine-augite, plates of ilmenite (up to 15 cm in diameter), prismatic crystals (up to 8 cm long) and

radiated aggregates of astrophyllite, tabular crystals of phlogopite (up to 20 cm in diameter), crystals of danalite–gentgelvite (up to 15 cm in diameter), almandine (up to 3 cm in diameter) and zircon (up to 3 cm long). Within the marginal zone of the REE-rich granite, accessory minerals of pegmatites also include typical REE-bearing accessories of this rock: chevkinite-(Ce), fergusonite-(Y), britholite-(Ce), REE-rich fluorapatite and fluorite, bastnäsite-(Ce), etc. Pegmatites of the central part of the massif have no REE mineralization.

REE-bearing minerals

A series of minerals is listed in a descending order of priority for REE budget contribution as follows: chevkinite-(Ce), chevkinite-like phases and products of metamict decay of chevkinite; bastnäsite-(Ce); allanite-(Ce); fergusonite-(Y); monazite-(Ce); britholite-(Y) and products of its metamict decay; thorite; apatite; titanite; pyrochlore group minerals and xenotime-(Y).

Chevkinite-(Ce), $(Ce,La,Ca,Th)_4(Fe^{2+},Mg)(Fe^{2+},Ti,Fe^{3+})_2(Ti,Fe^{3+})_2(Si_2O_7)_2O_8$ (Table 2), is a rare accessory mineral of peralkaline granites (Fig. 5) where its small (up to 0.7 mm) grains occur in interstices of rock-forming minerals. In pegmatites related to REE-rich peralkaline granites, this mineral forms small (up to 200 μm) zoned grains rimmed by aegirine. There are also smaller (up to 30 μm) inclusions of chevkinite-(Ce) in ferrorichterite (together with titanite and monazite-(Ce)) and ilmenite (together with fluorapatite). All analyzed grains of this mineral were metamict. Irregularly shaped or rounded grains of chevkinite-(Ce) are fractured, amorphous and irregularly zoned, with comparatively homogeneous Ln- and Fe-rich core (Fig. 7B), and deeply altered cation-deficient marginal zone. Such alteration often spreads over the whole grain producing compositionally fluctuating phases containing about 50 wt. % of $CaO+REE_2O_3$, 20 wt. % of TiO_2, 15 wt. % of SiO_2 and 15 wt. % of FeO. The average chemical composition of comparatively "fresh" chevkinite-(Ce) corresponds to the formula $(Ce_{1.57}La_{0.81}Nd_{0.52}Ca_{0.45}Y_{0.16}Pr_{0.15}Sm_{0.08}Th_{0.07}Gd_{0.06}Dy_{0.03}Sr_{0.02})_{\Sigma 3.92}(Fe^{2+}_{1.87}Mn_{0.03})_{\Sigma 1.90}(Ti_{2.85}Nb_{0.08}Al_{0.02})_{\Sigma 2.95}[Si_4O_{14}]O_{7.51}$.

Bastnäsite-(Ce), $Ce[CO_3]F$ (Table 2), is a widespread secondary mineral of peralkaline granites; while *bastnäsite-(La)*, $La[CO_3]F$, is found only in one sample of this rock. Both minerals form symplectites with ilmenite (Fig. 7C) and zircon, thin (up to 10 μm) veinlets along grain boundaries of rock-forming and accessory minerals, fill fractures within these grains and replace metamict chevkinite-(Ce) and pyrochlore (together with zircon, rutile, magnetite, ilmenite and chlorite). Chemical composition of bastnäsite-(Ce/La) varies widely, e.g. Ca-rich

margins appear rarely (Fig. 7C). Average chemical formula of bastnäsite-(Ce/La) is $(Ce_{0.37}La_{0.29}Nd_{0.16}Ca_{0.08}Pr_{0.06}Y_{0.04}Sm_{0.03}Gd_{0.01}Dy_{0.01}Ba_{0.01})_{\Sigma=1.06}[CO_3](F_{0.82}OH_{0.18})$.

Allanite-(Ce), $CaCeFe^{2+}Al_2[SiO_4][Si_2O_7]O(OH)$ (Table 2), is an important mineral of LREE in REE-rich peralkaline granites of Mt. Yumperuaiv where it forms irregularly shaped to oval grains (length is up to 5 mm, Fig. 7D) with numerous fractures and cavities filled with bastäsite-(Ce), xenotime-(Y) and goethite. Other associated minerals are zircon, fergusonite-(Y), thorite, titanite, pyrophanite, rutile, magnetite and fluorapatite. Grains of allanite-(Ce) have very inhomogeneous composition: they consist of separate blocks (1–100 μm) with widely varying contents of REEs, Ca, Fe, Al and Si. Average chemical composition of allanite-(Ce) corresponds to the formula $(Ca_{0.95}Na_{0.02})_{0.97}(Ce_{0.45}La_{0.24}Nd_{0.13}Ca_{0.05}Pr_{0.04}Sm_{0.02}Y_{0.01}Dy_{0.01})_{\Sigma0.95}(Fe^{2+}_{0.77}Mn_{0.08}Mg_{0.05}Zn_{0.04})_{\Sigma0.94}(Al_{1.31}Fe^{3+}_{0.52}Ti_{0.06})_{\Sigma1.89}[Si_3O_{11}](O_{0.33}OH_{1.67})_{\Sigma2.00}$. Metamict grains became sufficiently richer in Fe due to REEs (mainly La and Ce) and Si.

Fergusonite-(Y), $YNbO_4$ (Table 2), is a typical accessory, occasionally minor rock-forming mineral of the REE-rich Keivy peralkaline granites and associated pegmatites. In the Keivy massif it usually forms small (up to 30 μm) rounded inclusions in grains of quartz, zircon and chevkinite-(Ce) as well as chains of oval grains (up to 500 μm long) rimmed by annite along grain boundaries of quartz, microcline-perthite, magnetite and zircon. In pegmatites, fergusonite-(Y) occurs together with zircon, thorite, britholite-(Y), REE-rich fluorapatite, bastnäsite-(Ce), and ilmenite (Fig. 7A). Its spindle-like crystals (up to 1 mm long) have Y-rich core and fractured marginal zone with higher content of Ln, U, Th and P. Average chemical composition of fergusonite-(Y) corresponds to the formula $(Y_{0.64}Dy_{0.07}Gd_{0.05}Er_{0.05}Yb_{0.05}Pb_{0.04}Nd_{0.03}Ca_{0.03}Sm_{0.02}U_{0.02}Ce_{0.01}Ho_{0.01}Mn_{0.01}Th_{0.01})_{\Sigma1.04}(Nb_{0.91}Ti_{0.04}Ta_{0.02}Fe_{0.02}Si_{0.01})_{\Sigma1.00}O_4$.

Monazite-(Ce), *monazite-(La)* and *monazite-(Nd)*, $Ln[PO_4]$ (Table 2), are typical accessory minerals of peralkaline granites. Their content depends on REE amount in the rock. In the Keivy massif monazite-(Ce) is comparatively widespread in the form of irregularly shaped to rounded grains (up to 0.5 mm in diameter) occurring along quartz and microcline-perthite grain boundaries, in close association with zircon, rutile and goethite. Occasionally monazite-(Ce) forms small (up to 30 μm in diameter) inclusions in grains of Na-(Ca)-amphyboles. Monazite-(La) fills fractures (up to 5 μm thick) and cavities (up to 20 μm in diameter) in fluorapatite (Fig. 7E), ilmenite and ferrorichterite grains. Similarly, monazite-(Nd) occurs as rounded inclusions (up to 10 μm in diameter) in fluorapatite, and as close intergrowths with xenotime-(Y). Chemical compositions of monazite group of minerals is represented by the average formula $(La_{0.27}Ce_{0.35}Nd_{0.21}Pr_{0.07}Y_{0.05}Ca_{0.04}Sm_{0.04}Th_{0.02}Eu_{0.01})_{\Sigma1.06}[(P_{0.97}Si_{0.03})_{\Sigma1.00}O_{4.06}]$.

Britholite-(Y), $(CaCe)Y_3[SiO_4]_3O$, is a typical accessory mineral of the REE-rich Keivy peralkaline granites, where it usually forms thin (thickness is up to 100 μm) rims around REE-rich fluorapatite grains. In pegmatites, both phosphates give concentrically zoned segregations, where cores of fluorapatite are rimmed by britholite-(Y), thorite, fergusonite-(Y), zircon and a metamict compound of Ca, Ln, Y, Th, U and Pb (Fig. 7A). The last one, probably, appears due to U-Th-rich britholite alteration. Tiny (up to 5 μm) inclusions of britholite-(Y) are widespread also within fluorapatite, zircon and ilmenite grains. Chemical composition of comparatively fresh grain of britholite-(Y) with the mean content of REE sum is shown in Table 2. On the average, it corresponds to the formula $(Y_{1.82}Ca_{1.19}Fe_{0.48}Nd_{0.25}Dy_{0.22}Gd_{0.21}Th_{0.20}Ce_{0.18}Sm_{0.15}Er_{0.13}Yb_{0.12}Pb_{0.11}Mn_{0.07}La_{0.04}Pr_{0.02}U_{0.02})_{\Sigma 5.21}[SiO_4]_3O$.

Thorite, $Th[SiO_4]$ (Table 2), occurs in both REE-rich and ordinary peralkaline granites. In the ordinary ones, it forms the smallest (up to 5 μm in diameter) inclusions in about 30% of zircon grains. In REE-rich Keivy granites and associated pegmatites, thorite occurs as inclusions in zircon and fergusonite-(Y) grains, and as separate irregularly shaped grains (up to 0.5 mm in diameter, Fig. 7A,D) in the assemblages with fergusonite-(Y), britholite-(Y), fluorapatite, zircon and ilmenite. These grains are metamict and zoned due to the fact that in marginal areas Pb content increases instead of Th and U content. Average composition of thorite corresponds to the formula $(Th_{0.84}U_{0.08}Y_{0.07}La_{0.01}Ce_{0.04}Nd_{0.01})_{\Sigma 1.23}[(Si_{0.99}Al_{0.01})_{\Sigma 1.00}O_{4.03}]$.

Fluorapatite $Ca_5[PO_4]_3F$ (Table 2), is a widespread accessory mineral of both REE-rich and ordinary peralkaline granites, where it usually forms rounded inclusions (up to 0.6 mm in diameter) in ferrorichterite, quartz and ilmenite, as well as oval to irregularly shaped grains (up to 2.8 mm in diameter, Fig. 7E) in interstices between grains of rock-forming minerals and close intergrowths with amphyboles, titanite and ilmenite. In REE-rich peralkaline granites, fluorapatite grains often contain numerous small (up to 50 μm in diameter) inclusions of zircon, monazite-(La), xenotime-(Y) and britholite-(Ce). The last mineral also fills thin fractures in fluorapatite grains (see Fig. 7E). These grains usually have thin marginal zones depleted of REEs in comparison with core zones. In REE-rich granites, there are fluorapatite crystals consisting of separate blocks with different REE content. Chemical compositions of fluorapatite corresponds to the average formula $(Ca_{4.77}Na_{0.09}Y_{0.07}Ce_{0.04}Nd_{0.03}Sr_{0.02}La_{0.02}Fe_{0.01})_{\Sigma 5.05}[(P_{2.86}Si_{0.14})_{\Sigma 3.00}O_{12}](F,OH)_{1.03}$. In average, fluorapatite contains about 5.69 wt. % of REE_2O_3, and La/Ce relation does not change with total REE content growth (Fig. 8). Formation of REE-rich peralkaline granites is not accompanied by REE content growth in fluorapatite, and fluorapatite content in the rock.

Titanite, $CaTi[SiO_4]O$ (Table 2), is a common accessory mineral of peralkaline granites that has typical sphenoidal or irregularly shaped grains (up to 3 mm) in constant association with ferrorichterite, aegirine, fluorapatite and ilmenite. These grains are zoned usually due to iron content increase from core to marginal zones. In addition, there are rounded inclusions of titanite (up to 100 μm in diameter) in ilmenite grains. In contrast to fluorapatite, chemical composition of titanite depends on rock type. The mineral from REE-rich granites is enriched in Ln due to substitution $Na^{+}Ln^{3+} \leftrightarrow 2Ca^{2+}$. The average chemical composition of titanite corresponds to the formula $(Ca_{0.93}Na_{0.05}Y_{0.02}Ce_{0.01})_{\Sigma 1.01}$ $(Ti_{0.91}Fe_{0.08}Al_{0.03})_{\Sigma 1.02}$ $[Si_{1.02}O_5]$.

Pyrochlore group minerals, $(Na,Ca,REE)(Nb,Ti)_2O_6(OH,F)$ (Table 2), are rare accessory minerals of REE-rich peralkaline granites. Dominant *pyrochlor*e forms thin (diameter is up to 5 μm) lamella in ilmenite grains, as well as separate zoned cubic crystals (up to 400 μm in diameter, Fig. 7F) within microcline aggregates. *Ceriopyrochlore-(Ce)* occurs as small (diameter is up to 50 μm) irregularly shaped grains in close intergrowth with zircon. *Yttropyrochlore-(Y)* has inhomogeneous isometric grains (diameter is up to 30 μm) associating with zircon, titanite, fluorapatite, magnetite, xenotime-(Y) and bastnäsite-(Ce). Very rarely *plumbopyrochlore* occurs as fractured rounded grains (up to 100 μm) in constant assemblage with zircon and bastnäsite-(Ce). *Betafite* is found in REE-rich peralkaline granites as small (diameter is up to 80 μm) irregularly shaped zonal grains. They are always metamict and cation-deficient in Ca-position. Chemical compositions of these minerals are represented by the average formula $(Ca_{0.31}Y_{0.24}Ce_{0.11}Nd_{0.08}Pb_{0.06}La_{0.03}Dy_{0.03}U_{0.03}Mn_{0.02}Sm_{0.02}Th_{0.02}Sr_{0.01}Er_{0.01}Yb_{0.01})_{\Sigma 0.98}(Nb_{1.07}Ti_{0.40}$ $Si_{0.28}Fe_{0.21}Ta_{0.03}Al_{0.01})_{\Sigma=2.00}(O_{4.47}OH_{2.53})_{\Sigma 7.00}$.

Xenotime-(Y), $Y[PO_4]$ (Table 2), is a typical accessory mineral of both REE-rich and ordinary peralkaline granites that forms the smallest separate rounded or irregularly shaped grains (up to 150 μm, Fig. 7F) in association with titanite, fluorapatite, magnetite, fergusonite-(Y), monazite-(Nd), thorite and bastnäsite-(Ce). Its inclusions are also found in fluorapatite. Average chemical composition of xenotime-(Y) corresponds to the formula $(Y_{0.73}Dy_{0.07}Er_{0.05}Yb_{0.04}Gd_{0.03}$ $Ca_{0.02}Th_{0.02}Ce_{0.01}Pr_{0.01}Nd_{0.01}Sm_{0.01}Tb_{0.01}Ho_{0.01}Tm_{0.01}Lu_{0.01}U_{0.01})_{\Sigma 1.05}$ $[(P_{0.98}$ $Si_{0.04})_{\Sigma 1.02}O_4]$.

Aeschynite-(Y), $Y(TiNb)O_6$ (Table 2), is found in REE-rich peralkaline granites as small (up to 40 μm) irregularly shaped grains filling interstices between albite and quartz grains, in association with zircon, bastnäsite-(Ce) and magnetite. Aeschynite-(Y) grains always contain the smallest (up to 5 μm in diameter) inclusions of zircon. Average chemical composition of aeschynite-(Y) corresponds to the formula $(Y_{0.37}Ca_{0.13}Ce_{0.06}Nd_{0.06}Dy_{0.06}$ $Mn_{0.05}Pb_{0.05}Sm_{0.04}Gd_{0.04}Er_{0.04}Th_{0.04}U_{0.02}La_{0.01}Pr_{0.01})_{\Sigma 0.98}$ $(Ti_{0.90}Nb_{0.67}Fe_{0.22}Si_{0.20}Zr_{0.01})_{\Sigma 2.00}$ $(O_{5.22}$ $OH_{0.78})_{\Sigma 6.00}$.

Probably, the list of REE-bearing minerals in peralkaline granites is not exhausted by the above phases. In addition to the abovementioned britolite- and chevkinite-like phases, this rock contains other amorphous compounds of REE, Th, U, Pb, Ca, Fe and Si closely associated with zircon, rutile and bastnäsite-(Ce). Volume fraction of such phases can reach 30% of the total volume of REE-bearing accessories in peralkaline granites.

Geochemistry

Geochemically, REE-rich granite slightly differs from ordinary granite. In the scatter plot "total alkali vs silica", sample points form two partly overlapping fields (Fig. 9): ordinary peralkaline granite is characterized by increased content of total alkali and a wide distribution of silica content. REE-rich granite is characterized by reduced total alkali. Besides alkali, ordinary granite is characterized by a relative increase of Ca and Al content. REE-rich granite is also essentially enriched by Fe^{3+} and Zr, and, to a lesser degree, by TiO_2, MgO and MnO (Fig. 10, Table 3). According to microprobe analyses, chemical composition of felsic rock-forming minerals is identical in both REE-rich and ordinary varieties of peralkaline granite. The difference in chemical composition of REE-rich granite is caused by feldspar/quartz proportion decrease, increase of alkalinity of clinopyroxenes (aegirine-augite to aegirine, Fig. 11), and by significant growth of zircon content (up to 5 vol. %) and REE minerals. All analyzed zircons are REE-free. Good REE/Zr correlation as well as textural relationships in granite reflect paragenetic link between zircon and REE-bearing minerals (Fig. 12).

Both LREE and HREE amounts linearly grow with increase of total REE content (Fig. 13). Chondrite-normalized REE patterns of REE-rich and ordinary granites demonstrate a similar behavior: a steep LREE profile, a clear Eu negative anomaly, and a near-horizontal HREE profile (Fig. 14A, B). LREE part of chondrite-normalized REE pattern of gneiss adjoining peralkaline granites is similar to that of ordinary granites, and differs by the absence of Eu minimum and relative depletion with HREE (Fig. 14A).

Normalization of REEs in REE-rich granites and pegmatites by ordinary, parental granite is a suitable method of REE distribution estimation during magmatic and post-magmatic evolution of the peralkaline granite massif. The REE pattern normalized with this method is shown in Figure 14C, demonstrating relative depletion of REE-rich granite with HREE, and Eu negative anomaly. The wide field of the REE pattern is caused by gradual transition from ordinary to REE-rich granite. With increase of REE concentration, the LREE become predominant over HREE, and the negative Eu anomaly becomes more intensive. Normalization

by ordinary granite of REE-rich pegmatite-like peralkaline granite bodies shows an opposite pattern: HREE distinctly prevail over LREE; herewith, sharp increase of REE content from Eu to Tm is replaced with the same sharp concentration decrease from Tm to Lu (Fig. 14D).

Discussion

Peralkaline and alkaline igneous complexes are highly enriched in REE, in particular, HREE and HFSE, notably Zr, Ti, and Nb. High alkali (and fluorine) content in the corresponding melts leads to their depolymerization, decrease in solidus temperature, and reduction of the melts viscosity. All these factors promote incorporation of the above metals in these magmas (Manning, 1981; Linnen and Keppler, 2002; Thomas et al., 2012; Bartels et al., 2013). Particularly, high content of Na and K in a high- to medium temperature silicate melt increases solubility of HFSE and REE due to formation of polymeric alkali-silicate and alkali-fluorine complexes (Watson, 1979; Collins et al., 1982; Salvi and Williams-Jones, 2005). Besides, this causes increase of non-bridging oxygen fraction in the melt, which in turn allows to introduce HFSE and REE in the melt structure (Peiffert et al., 1996). Both REE and HFSE are incompatible elements concentrating in the residual melt.

Late magmatic/postmagmatic behavior of these metals is also determined by alkalinity: pH increase leads to precipitation of REE and HSFE, while acidic condition stabilizes them in the solution (Migdisov et al., 2016). Therefore, estimation of alkali content in residual melt/fluid/solution can help us to understand genetic features of REE-mineralization formation.

Average composition of peralkaline granite of the Western Keivy massif was regarded as chemical composition of initial magma (Table 3). Sequence of crystallization of the main rock-forming minerals, Qz → Qz+Ab → Ab+Mi → Px+Amf (Table 4), and volume proportion of each mineral were estimated in thin sections. It was taken into account that significant part of arfvedsonite crystallized on the autometasomatic/hydrothermal stage as rims around clinopyroxene grains (Fig. 4C). Composition of residual peralkaline granite melt at each stage of the rock formation was estimated as difference between the melt composition at previous stage and composition of precipitated minerals (Table 4 and Fig. 15).

The results showed that consecutive precipitation of quartz, albite and microcline causes gradual decrease of silica content. However, crystallization of mafic minerals significantly changes the melt composition: sharp decrease of silica content and sharp increase of K content. As a result, incompatible HFSE and REE accumulating in acidic melt of the early–medium stages (stages 0-4 in Fig. 15), is carried to high-alkaline residual melt/postmagmatic solution (stages 5-6 in Fig. 15) and immediately precipitate as zircon and REE-minerals. Crystallization

of REE-bearing minerals (and partly zircon) soon after mafic minerals is confirmed by close spatial association of these minerals in the rock (compare Fig. 16 and 5).

We discovered that contacts of REE-bearing minerals with mafic minerals occur three times as often as contacts with quartz, albite or microcline (Fig. 16). Therefore, we concluded that most REE minerals (partly exclude monazite-(Ce), fluorapatite and titanite) crystallized within late magmatic stage (stages 5-6 in Fig. 15) or later (e.g. bastnäsite-(Ce) forms fibers in other REE minerals (Fig. 7D), pyroxenes and amphiboles). High content of iron in the late alkaline melt/solution (stage 5-6 in Fig. 15) leads to co-precipitation of magnetite. We noted a relatively intensive development of thin films of iron (hydro)oxydes along boundaries of rock-forming minerals grains (e.g. see Fig 4B).

It is important that crystallization of quartz and silicates cause significant decrease of silica content in the residual melt and, consequently, decrease of viscosity. In turn, low viscosity of residual melt leads to its mobility along P-T gradient within cooling intrusive. Since content of mafic minerals in peralkaline granite gradually increases from internal parts of the massif to its contact with host gneiss (see Fig. 3), we suggest that late residual solution enriched in Fe, HFSE and REE, migrated from a comparatively hot core of the massif to its cooler margins.

Since HREE are less sensitive to alkalinity growth and temperature decrease than LREE, migrating residual melt increased HREE/LREE separation. Therefore, marginal REE-rich parts of the granite massif are also HREE-rich with most of HREE carried out from granites to pegmatites. Pegmatites formed just after crystallization of the granite massif. Pegmatites located in marginal parts of the massif became enriched in HREE.

Residual melt appeared to be relatively rich in water and fluorine. This fact is proved by widely spread water-containing minerals (phlogopite, amphiboles and others) and fluorite in pegmatites. Presence of characteristic graphite globules proves acidic environment (reducing condition) of pegmatite origin.

Conclusions

1. Zones of REE and Zr enrichment (so called “REE-rich” granite) in the Western Keivy peralkaline granite massif are associated with marginal and apical parts. Some of these zones are potentially economic in terms of REE and Zr (namely, the Yumperuaiv and Large Pedestal deposits).
2. Rock-forming minerals have the following crystallization sequence: quartz – albite – microcline – alkali pyroxenes and amphiboles. Mafic minerals crystallizing at the late magmatic stage change composition of residual liquid significantly. Silica content

sharply decreases and potassium content increases by order of magnitude. Since REE solubility under high-alkali conditions is very low, REE minerals precipitate. Thus, crystallization of alkali mafic minerals triggers REE minerals precipitation.

3. Since silica content in the late magmatic liquid drops, its mobility sharply increases. So, the liquid easily migrates to apical and marginal parts of the massif.
4. The main minerals concentrating REE are chevkinite-(Ce) and chevkinite-like phases, bastnäsite-(Ce); allanite-(Ce); fergusonite-(Y); monazite-(Ce). Fergusonite-(Y) and non-diagnosed amorphous phases probably being a product of alteration of britholite-(Y) are principal minerals of HREE. The main REE concentrators are different for different deposits and occurrences.
5. In cognate quartz-rich pegmatites, HREE prevails over LREE. Relative fraction of HREE in REE sum is about 88%.

Acknowledgements

This research was supported by the Presidium of the Russian Academy of Sciences (Programs No 27), the Russian Foundation for Basic Research and the Murmansk Region Government (Grant 12-05-98802), and Laplandia Minerals Ltd. (Apatity, Russia). We thank V.G. Zaitsev (FGU TFGI, Apatity) for unpublished materials; Dr. Yu.S. Polekhovsky, T.L. Panikorovsky (Saint-Petersburg State University), Dr. N.G. Konopleva (NRC KSC RAS), Ye.N. Fomina (GI KSC RAS), and V.G. Panikorovskaya for assistance in fieldworks; Prof. P.M. Goryainov (GI KSC RAS) and Dr. N.G. Konopleva (NRC KSC RAS) for discussion. The detailed comments by anonymous reviewers helped us to improve this paper significantly.

References

Balagansky, V.V., Basalaev, A.A., Belyaev, O.A., Pozhilenko, V.I., Radchenko, A.T., and Radchenko, M.K., 1996, Geological map of Kola region 1:500000. Apatity, GI KSC RAS (in Russian).

Bartels, A., Behrens, H., Holtz, F., Schmidt, B.C., Fechtelkord, M., Knipping, J., Crede, L., Baasner, A., and Pukallus, N., 2013, The effect of fluorine, boron and phosphorus on the viscosity of pegmatite forming melts. Chem. Geol. 346, 184–198. doi: 10.1016/j.chemgeo.2012.09.024

Batieva, I.D, 1976. Petrology of alkaline granitoids of the Kola Peninsula. Leningrad, Nauka, 224 p. (in Russian).

Boynton, W.V., 1984. Cosmochemistry of the rare earth elements: meteorite studies. In: Henderson P. (ed.) Rare earth element geochemistry. Elsevier. P 63-114.

Chakhmouradian, A.R., Smith, M.P., Kynicky, J., 2015. From "strategic" tungsten to "green" neodymium: A century of critical metals at a glance. Ore Geol. Rev. 64, 455–458. doi:10.1016/j.oregeorev.2014.06.008

Chukhina, T.S., et al., 1963, Report on revision survey of rare earths and rare metals, carried out in 1962 in the north-western Keivy area, the Lovozero District of the Murmansk Region. Unpublished report, Apatity, Russia, Federal State Office "Territorial Foundation of Geological Information of Northwestern Federal District" (FGU TFGI SZFO), (in Russian).

Collins, W.J., Beams, S.D., White, A.J.R., Chappell, B.W., 1982. Nature and origin of A-type granites with particular reference to southeastern Australia. Contrib. to Mineral. Petrol. 80, 189–200. doi:10.1007/BF00374895

Gaskelberg, L.A., Luk'yanova, N.V., Gaskelberg, V.G., Barzhitsky, V.V., Snyatkov, A.B., Belolipetsky, A.P., Zaitsev, V.G., Antonyuk, E.S., Remizova, A.M., and Ilyin, Yu.I. (1978) Joint report on supplementary geologic investigation of Keivy structure and composition of new geologic map of scale 1:200000. Unpublished report, Apatity, Russia, Federal State Office "Territorial Foundation of Geological Information of Northwestern Federal District" (FGU TFGI SZFO), (in Russian).

Ishihara, S., Hua, R., Hoshino, M., Murakami, H., 2008. REE Abundance and REE Minerals in Granitic Rocks in the Nanling Range, Jiangxi Province, Southern China, and Generation of the REE-rich Weathered Crust Deposits. Resour. Geol. 58, 355–372. doi:10.1111/j.1751-3928.2008.00070.x

Kalashnikov, A.O., Konopleva, N.G., Pakhomovsky, Y.A., Ivanyuk, G.Y., 2016. Rare Earth Deposits of the Murmansk Region, Russia—A Review. Econ. Geol. 111, 1529–1559. doi:10.2113/econgeo.111.7.1529

Kharitonov, L.Ya. (ed.), 1958. Geology of the USSR. Vol. 27. Murmansk Region. Part 1. Moscow, Gosgeoltekhizdat. 714 p. (in Russian).

Konopleva, N.G., Ivanyuk, G.Yu., Pakhmovsky, Ya.A., Yakovenchuk, V.N., Kalashnikov, A.O., Mikhailova, J.A., Goryainov, P.M., 2012. Resourse potential of the Kola Rare Earth Province. Proceedings of the IX Fersman's scientific session. K&M, Apatity, pp. 332-334. URL http://geoksc.apatity.ru/images/stories/Print/Fersman_2012.pdf (in Russian).

Kozlov, N.E., Sorokhtin, N.O., Glaznev, V.N., Kozlova, N.E., Ivanov, A.A., Kudryashov, N.M., Martynov, E.V., Tyuremnov, V.A., Matyushkin, A.V., and Osipenko, L.G., 2006, Geology of Archaean of the Baltic Shield: Saint-Petersburg, Nauka, 329 p. (in Russian).

Kupletsky, B.M., and Vorobyova, O.A., 1930, Geological and petrographic observations

on the central watershed of Kola Peninsula in summer of 1928 year. Trudy Leningradskogo obshchestva estestvoispytateley, Geology and mineralogy, v. 9 (in Russian).

Le Maitre, R.W. (Ed.), 2002. Igneous Rocks. A Classification and Glossary of Terms. Recommendations of the International Union of Geological Sciences Subcommission on the Systematics of Igneous Rocks. Cambridge University Press, New York.

Linnen, R., and Keppler, H., 2002, Melt composition control of Zr/Hf fractionation in magmatic processes: Geochim. Cosmochim. Acta, 66, 3293–3301. doi:10.1016/S0016-7037(02)00924-9

Manning, D.A.C., 1981, The effect of fluorine on liquidus phase relationships in the system Qz-Ab-Or with excess water at 1 kb. Contrib. Mineral. Petrol. 76, 206–215. doi: 10.1007/BF00371960

Migdisov, A., Williams-Jones, A.E., Brugger, J., Caporuscio, F.A., 2016. Hydrothermal transport, deposition, and fractionation of the REE: Experimental data and thermodynamic calculations. Chem. Geol. 439, 13–42. doi:10.1016/j.chemgeo.2016.06.005

Miller, R.R., 1986. Geology of the Strange Lake akalic complex and the associated Zr-Y-Nb-Be-REE mineralization. Report 86-1. P. 11-19. Newfoundland Department of Mines and Energy. Mineral Development Division.

Mitrofanov, F.P., Zozulya, D.R., Bayanova, T.B., Levkovich, N. V., 2000. The World's Oldest Anorogenic Alkaline Granitic Magmatism in the Keivy Structure on the Baltic Shield. Dokl. Earth Sci. 374, 1145–1148.

Morimoto, N., 1988. Nomenclature of Pyroxenes. Mineral. Petrol. 39, 55–76. doi:10.1007/BF01226262

Peiffert, C., Nguyen-Trung, C., Cuney, M., 1996. Uranium in granitic magmas: Part 2. Experimental determination of uranium solubility and fluid-melt partition coefficients in the uranium oxide-haplogranite-H_2O-NaX (X = Cl, F) system at 770°C, 2 kbar. Geochim. Cosmochim. Acta 60, 1515–1529. doi:10.1016/0016-7037(96)00039-7

Porotova, G.A., Sipakova, M.S., and Zilberman R.S., 1959. Report on Kol'skaya aerial geophysical party works on the Murmansk Region territory. Unpublished report, Apatity, Russia, Federal State Office "Territorial Foundation of Geological Information of Northwestern Federal District" (FGU TFGI SZFO), 231 p. (in Russian).

Thomas, R., Davidson, P., and Beurlen, H., 2012. The competing models for the origin and internal evolution of granitic pegmatites in the light of melt and fluid inclusion research. Mineral. Petrol. 106, 55–73. doi:10.1007/s00710-012-0212-z

Vetrin, V.R., Rodionov, N. V., 2009. Geology and geochronology of neoarchean anorogenic magmatism of the Keivy structure, Kola Peninsula. Petrology 17, 537–557.

doi:10.1134/S0869591109060022

Salvi, S., Williams-Jones, A.E., 2005. Alkaline granite-syenite deposits, in: Linnen, R.L., Samson, I.M. (Eds.), Rare-Element Geochemistry and Mineral Deposits: Geological Association of Canada, GAC Short Cource Notes 17. pp. 315–341.

Watson, E.B., 1979. Zircon saturation in felsic liquids: Experimental results and applications to trace element geochemistry. Contrib. Mineral. Petrol. 70, 407–419. doi: 10.1007/BF00371047

Figure captions

Fig. 1. Geology of the Murmansk Region (A - simplified after Balagansky et al., 1996), and the Western Keivy peralkaline granite massif (B - simplified after Gaskelberg et al., 1978).

Fig. 2. Contact of the REE-rich granite and host gneiss at Mt. Large Pedestal. A – general view, B – detailed view.

Fig. 3. Brief overview of the Western Keivy peralkaline granite. I – General scheme of gradual transition from massive (dark orange) to gneissose (light orange) peralkaline granite. Colors correspond to Fig. 1B. II – Typical varieties of granite (polished thin section in transmitted light). Ab – albite, Aeg – aegirine, Arf – arfvedsonite, Mc – microcline, Qz – quartz, Zrn – zircon. III – Average grain size of rock-forming minerals. IV – Percentage of mafic minerals. V – Average radioactive background.

Fig. 4. Relationships of minerals in peralkaline granites (ordinary variety). BSE images. A – sequence of formation of rock-forming minerals. Decrease of idiomorphism of felsic minerals: rounded and euhedral quartz – subhedral albite – subhedral to anhedral microcline – anhedral to intersticial aegirine. B – simultaneous crystallization of aegirine and arfvedsonite. Note that zircon predominantly contacts with mafic minerals and forms inclusions in it. C – alteration of aegirine-augite with arfvedsonite and titanite. D – zircon and monazite-(Ce), main HFSE and REE minerals of ordinary granite. Note that zircon grains occur along fractures, and monazite-(Ce) fills in interstices of rock-forming minerals. Ab – albite, Aeg – aegirine, Aeg-Au – aegirine-augite, Ap – fluorapatite, Arf – arfvedsonite, Baf – bafertisite, Gth – goethite, Hem – hematite, Ilm – ilmenite, Mc – microcline, Mnz – monacite-(Ce), Ttn – titanite, Qz – quartz, Zrn – zircon.

Fig. 5. Sequence of mineral formation in peralkaline granite of the Western Keivy massif.

Fig. 6. Granitic pegmatite within ordinary granites at Mt. Large Pedestal. A – general view, B – detailed view. Gr – graphite, Qz – quartz.

Fig. 7. Relations between REE-bearing minerals in pegmatite of Mt. Maly Pedestal (A) and peralkaline granites of Mts Large Pedestal (B), Maly Pedestal (C), Yumperuaiv (D, F) and the Rovozero Lake region (E). Ab – albite, Aeg – aegirine, Aln – allanite-(Ce), Ap – fluorapatite, Btl – britholite-(Y), Bsn – bastnäsite-(Ce), Bsn' – Ca-rich bastnäsite-(Ce), Chk – chevkinite-

(Ce), Chk' – altered chevkinite-(Ce), Frct – ferrorichterite, Frg – fergusonite-(Y), Ilm – ilmenite, Gth – goethite, Mag – magnetite, Mc – microcline, Mnz – monazite-(La), Pcl – pyrochlore, Pcl' – altered pyrochlore; Qz – quartz, Thr – thorite, Xtm – xenotime-(Y), Zrn – zircon.

Fig. 8. Scatterplots of lanthanoid sum (Ln_2O_3) vs La_2O_3 and Ce_2O_3 in fluorapatite of the peralkaline granites.

Fig. 9. Alkali sum vs silica scatterplot for peralkaline granites.

Fig. 10. Comparison of average chemical composition of REE-rich and ordinary varieties of peralkaline granite. Whiskers are standard deviation.

Fig. 11. Classification diagram for clinopyroxenes of the Western Keyvy peralkaline granite massif. Aeg – aegirine, Aeg-Au – aegirine-augite, En – enstatite, Fs – ferrosilite, Jd – jadeite, Omp – omphacite, Wo – wollastonite (Morimoto, 1988).

Fig. 12. REE vs ZrO_2 in peralkaline granites.

Fig. 13. Total REE vs LREE and HREE in peralkaline granites.

Fig. 14. Chondrite-normalized REE pattern for host gneisses, ordinary (A) and REE-rich (B) varieties of peralkaline granites (chondrite by Boynton, 1984); REE pattern of REE-rich peralkaline granites (C) and related pegmatite (D), normalized by ordinary peralkaline granite.

Fig. 15. Evolution of liquid phase composition at magmatic stage of peralkaline granite formation (in accordance with Table 4).

Fig. 16. Frequency of contacts between grains of rock-forming and accessory REE-bearing minerals, and volume percent of rock-forming minerals (for massive peralkaline granites). Ab – albite, Amf – amphibole, Mc – microcline, Px – pyroxene, Qz – quartz.

Table 1. Parameters of analyses.

Element	Limit of accuracy for microprobe analyses, wt.%	Standards for WDS microprobe analyses	Limit of accuracy for wet chemistry analyses, wt.%
H_2O			0.01
Li_2O			0.00001
CO_2			0.1
F	0.5*		0.001
Na_2O	0.1	Lorenzenite	0.01
MgO	0.1	Pyrope	0.01
Al_2O_3	0.05	Pyrope	0.01
SiO_2	0.05	Diopside	0.01
P_2O_5	0.05	Fluorapatite	0.01
S_{total}			0.01
Cl			0.01
CaO	0.03	Diopside	0.01
K_2O			0.01
Sc_2O_3	0.02	Thortveitite	
TiO_2	0.02	Lorenzenite	0.01
V_2O_3	0.1	Metallic vanadium	
Cr_2O_3	0.02	Chromite	
MnO	0.01	Synthetic $MnCO_3$	0.01
Fe_2O_3			0.01
FeO	0.01	Hematite	0.1
CoO	0.01	Metallic cobalt	
NiO	0.01	Metallic nickel	
ZnO	0.01	Synthetic ZnO	0.01
Rb_2O			0.00001
SrO	0.1	Celestine	0.01
Y_2O_3	0.1	Synthetic $Y_3Al_5O_{12}$	
ZrO_2	0.1	Synthetic $ZrSiO_4$	0.01
Nb_2O_5	0.05	Metallic niobium	
Cs_2O			0.00001
BaO	0.05	Barite	
La_2O_3	0.05	Synthetic $LaCeS_2$	
Ce_2O_3	0.05	Synthetic $LaCeS_2$	
Pr_2O_3	0.1	$LiPr(WO_4)_2$	
Nd_2O_3	0.1	Synthetic $LiNd(MoO_4)_2$	
Sm_2O_3	0.1	Synthetic $LiSm(MoO_4)_2$	
Eu_2O_3	0.1	Synthetic $LiEu(MoO_4)_2$	
Gd_2O_3	0.1	Synthetic $LiGd(MoO_4)_2$	
Tb_2O_3	0.1	Synthetic $LiTb(MoO_4)_2$	
Dy_2O_3	0.1	Synthetic $LiDy(WO_4)_2$	
Ho_2O_3	0.1	Synthetic $LiHo(WO_4)_2$	
Er_2O_3	0.1	Synthetic $LiEr(MoO_4)_2$	
Tm_2O_3	0.1	Synthetic $LiTm(MoO_4)_2$	
Yb_2O_3	0.1	Synthetic $LiYb(MoO_4)_2$	
Lu_2O_3	0.1	Synthetic $LiLu(MoO_4)_2$	
HfO_2	0.2	Metallic hafnium	
Ta_2O_5	0.05	Metallic niobium	
PbO	0.1	Wlfenite	
ThO2	0.1	Torite	
UO2	0.1	Metallic uranium	

* Fluorine measured by EDS method.

Table 2. Chemical composition of REE minerals (wt. %, microprobe analyses).

Sample	Chevkinite-(Ce)	Bastnäsite-(Ce)	Bastnäsite-(La)	Allanite-(Ce)	Fergusonite-(Y)	Monazite-(Ce)	Monazite-(La)	Monazite-(Nd)	Britholite-(Y)	Thorite	Fluorapatite	Titanite	Pyrochlore	Ceriopyrochlore-(Ce)	Yttropyrochlore-(Y)	Plumbopyrochlore	Betafite	Xenotime-(Y)	Aeschynite-(Y)
SiO_2	17.25	–	–	30.88	0.12	0.67	0.87	–	22.08	15.66	–	30.76	3.73	3.98	7.60	1.52	1.02	0.90	1.81
TiO_2	21.67	–	–	0.13	0.81	–	–	–	–	–	–	34.31	11.47	9.48	4.21	2.04	30.84	–	22.53
Al_2O_3	–	–	–	12.56	–	–	–	–	–	–	–	1.08	–	0.79	–	–	–	–	–
Na_2O	–	–	–	–	–	–	–	–	–	–	–	0.63	–	–	–	–	–	–	–
CaO	2.36	0.16	1.23	9.99	0.33	–	3.09	1.92	13.52	3.30	52.41	26.17	7.87	3.74	4.45	5.53	3.16	–	0.45
MgO	–	–	–	0.49	–	–	–	–	–	–	–	–	–	–	–	–	–	–	–
FeO	6.34	–	–	16.09	–	–	–	–	2.70	–	–	2.23	3.94	7.65	2.53	6.60	5.11	–	7.48
MnO	–	–	–	0.28	–	–	–	–	–	–	–	0.11	–	–	1.11	–	0.54	–	1.61
SrO	0.39	–	–	–	–	–	–	–	–	–	0.65	0.10	–	–	–	–	–	–	–
P_2O_5	–	–	–	–	–	27.41	29.72	29.27	–	–	36.86	–	–	–	–	–	–	35.65	–
Nb_2O_5	0	–	–	–	47.76	–	–	–	–	–	–	–	45.51	44.72	37.25	39.90	23.83	–	31.65
Ta_2O_5	–	–	–	–	–	–	–	–	–	–	–	–	3.90	–	1.60	5.14	–	–	–
Y_2O_3	0.71	1.44	1.65	–	24.04	0.91	1.45	8.90	26.45	–	2.45	0.74	3.13	2.52	15.60	3.78	16.60	44.18	18.17
La_2O_3	12.44	18.88	26.61	6.97	–	17.95	25.51	18.92	1.86	2.63	0.23	0.25	1.54	3.30	1.36	2.83	–	–	0.36
Ce_2O_3	22.50	37.20	35.78	11.76	0.61	31.81	6.71	3.15	9.48	4.76	1.00	0.93	8.45	12.51	3.63	6.80	0.37	–	0.38
Pr_2O_3	2.42	3.99	3.90	1.22	–	3.82	7.61	5.65	1.64	–	0.22	0.29	–	–	–	–	–	–	–
Nd_2O_3	7.88	11.31	9.04	3.47	2.16	11.31	21.43	20.00	9.01	–	1.79	0.57	7.04	11.31	2.39	5.96	0.28	0.24	1.06
Sm_2O_3	2.42	2.37	2.10	0.54	2.13	2.42	3.54	5.34	2.84	–	–	–	1.88	–	1.31	2.01	–	0.52	0.94
Eu_2O_3	–	–	–	–	–	–	–	3.30	–	–	–	–	–	–	–	–	–	–	–
Gd_2O_3	–	0.36	–	–	3.39	–	–	3.56	3.36	–	–	–	–	–	2.12	2.43	–	1.86	1.68
Tb_2O_3	–	–	–	–	–	–	–	–	–	–	–	–	–	–	–	–	–	0.54	–
Dy_2O_3	–	–	–	–	5.21	–	–	–	3.50	–	–	–	–	–	4.04	4.03	1.10	3.50	2.19
Ho_2O_3	–	–	–	–	–	–	–	–	–	–	–	–	–	–	–	–	–	1.40	–
Er_2O_3	–	–	–	–	4.18	–	–	–	1.23	–	–	–	–	–	2.10	–	0.72	4.64	1.65
Tm_2O_3	–	–	–	–	–	–	–	–	–	–	–	–	–	–	–	–	–	0.63	–
Yb_2O_3	–	–	–	–	4.37	–	–	–	–	–	–	–	–	–	1.63	–	1.52	4.08	–
Lu_2O_3	–	–	–	–	–	–	–	–	–	–	–	–	–	–	–	–	–	0.68	–
PbO	–	–	–	–	–	–	–	–	–	12.22	–	–	–	–	3.20	11.42	3.27	–	3.76
ThO_2	3.63	–	–	–	2.42	3.71	–	–	–	61.44	–	–	1.54	–	2.90	–	2.67	–	1.75
UO_2	–	–	–	–	2.46	–	–	–	–	–	–	–	–	–	0.98	–	8.41	–	1.99
F	–	6.24	5.60	–	–	–	–	–	–	–	3.30	–	–	–	–	–	–	–	–
Σ	**100.01**	**81.95**	**85.91**	**94.38**	**99.99**	**100.01**	**99.93**	**100.01**	**97.67**	**100.01**	**98.91**	**98.17**	**100.00**	**100.00**	**100.01**	**99.99**	**99.44**	**98.82**	**99.46**

Chemical composition of fresh grain of each mineral with the mean content of REE sum is presented.

"–" is value below detection limit.

Table 3. Chemical composition of ordinary and REE-rich varieties of peralkaline granite of the Western Keivy massif.

	Ordinary variety (70 samples)					REE-rich variety (19 samples)				
	Mean	Median	Minimum	Maximum	Std.Dev.	Mean	Median	Minimum	Maximum	Std.Dev.
	wt.%									
SiO_2	73.23	73.06	68.23	77.88	1.74	73.42	73.56	67.91	77.03	2.17
TiO_2	0.37	0.38	0.13	0.57	0.08	0.48	0.42	0.26	1.37	0.25
ZrO_2	0.09	0.06	0.01	0.70	0.10	0.92	0.53	0.11	2.82	0.86
Al_2O_3	11.09	11.19	7.31	13.26	1.15	7.87	7.99	3.62	12.87	1.92
Fe_2O_3	1.25	0.94	0.00	5.15	1.09	5.20	5.58	2.43	7.39	1.52
FeO	3.37	3.37	1.59	5.04	0.72	3.69	3.68	2.21	6.58	1.10
MnO	0.07	0.07	0.02	0.14	0.02	0.11	0.10	0.06	0.18	0.04
MgO	0.041	0.030	0.000	0.360	0.054	0.052	0.040	0.000	0.200	0.043
CaO	0.407	0.355	0.000	1.370	0.244	0.294	0.370	0.000	0.530	0.188
SrO	0.028	0.020	0.020	0.100	0.017	0.027	0.020	0.020	0.100	0.019
Zn	0.021	0.020	0.011	0.059	0.009	0.072	0.070	0.023	0.160	0.035
Li_2O	0.0130	0.0120	0.0026	0.0270	0.0046	0.0067	0.0066	0.0005	0.0200	0.0055
Na_2O	4.16	4.18	0.27	5.49	0.59	2.81	2.34	0.91	5.40	1.37
K_2O	4.71	4.73	3.53	5.65	0.37	3.76	3.89	1.42	4.91	0.90
Cs_2O	0.00029	0.00029	0.00007	0.00063	0.00011	0.00027	0.00023	0.00010	0.00097	0.00020
Rb_2O	0.0222	0.0200	0.0095	0.0510	0.0081	0.0462	0.0440	0.0260	0.0780	0.0145
P_2O_5	0.0277	0.0200	0.0000	0.1700	0.0263	0.0237	0.0200	0.0000	0.0800	0.0214
H_2O^-	0.136	0.130	0.017	0.250	0.052	0.176	0.180	0.040	0.300	0.076
l.o.i.	0.512	0.490	0.180	1.470	0.180	0.478	0.510	0.070	0.760	0.180
F^-	0.053	0.056	0.004	0.120	0.028	0.036	0.024	0.008	0.120	0.030
Cl^-	0.01	0.01	0.01	0.06	0.01	0.01	0.01	0.01	0.03	0.01
CO_2	0.10	0.10	0.00	0.23	0.06	0.12	0.10	0.00	0.31	0.08
S_{total}	0.0641	0.0600	0.0200	0.2000	0.0294	0.0521	0.0500	0.0300	0.0900	0.0178

ppm										
La	38.2	31.5	7.0	209.7	32.5	643.8	448.1	123.9	2316.5	575.1
Ce	98.0	81.9	29.6	350.5	61.5	1423.1	1083.9	314.1	4970.5	1205.0
Pr	10.2	8.7	2.5	44.4	7.3	154.9	93.2	37.8	549.2	136.2
Nd	39.5	32.6	9.8	149.5	25.6	555.8	330.8	165.7	1847.6	470.7
Sm	8.4	7.2	2.4	26.0	4.7	119.4	63.6	35.2	428.0	110.8
Eu	0.9	0.8	0.2	2.1	0.4	8.8	6.3	2.6	30.3	7.9
Gd	9.2	8.3	2.7	28.2	5.1	134.7	91.1	40.1	493.9	126.2
Tb	1.4	1.2	0.5	4.1	0.7	19.9	14.9	5.8	67.3	17.6
Dy	9.0	7.6	3.1	24.9	4.8	128.6	96.5	34.0	436.5	114.1
Ho	1.8	1.6	0.6	5.1	1.0	24.6	19.5	6.9	76.4	20.6
Er	5.6	4.7	1.9	15.6	3.1	75.5	57.6	22.0	234.6	62.5
Tm	0.9	0.7	0.3	2.7	0.5	10.7	8.3	3.4	30.5	8.3
Yb	6.5	5.1	2.7	21.1	4.0	69.4	55.1	22.4	205.5	53.2
Lu	1.0	0.8	0.4	3.4	0.6	9.1	6.8	3.3	26.0	6.6
Y	41.5	35.0	10.1	104.0	21.4	585.7	381.3	152.8	2004.6	538.9
LREE	**195.0**	**166.0**	**60.0**	**675.3**	**119.4**	**2905.8**	**2021.1**	**694.3**	**10142.0**	**2487.7**
HREE	**76.8**	**65.6**	**25.7**	**206.4**	**39.9**	**1058.2**	**794.0**	**304.8**	**3575.5**	**938.6**
REE	**271.8**	**229.6**	**86.8**	**868.2**	**153.5**	**3964.0**	**2507.6**	**1271.5**	**13717.5**	**3341.6**

Mean – arithmetic mean; Std.Dev. – standard deviation; l.o.i. – loss on ignition.

LREE are La to Eu, and HREE are Gd to Lu plus Y.

SiO_2 to S_{total} analyses are wet chemistry, REE analyses are ICP MS.

Table 4. Evolution of composition of the peralkaline granitic magma/mush in terms of rock-forming minerals and oxides (coevolution of mineral composition of crystallized part and chemical composition of liquid phase).

	Stages						
	Initial composition	1	2	3	4	5	6
Phase composition of the magma/mush, vol. %							
Quartz	0	20	35	35	35	35	35
Albite	0	0	10	24	24	24	24
Microcline	0	0	0	10	20	28	28
Aegirine	0	0	0	0	0	3	7
Arfvedsonite	0	0	0	0	0	0	3
Liquid	100	80	45	31	21	10	3
Chemical composition of the liquid phase (wt. %)							
SiO_2	74.79	67.88	59.03	52.90	47.79	17.53	~0
Al_2O_3	10.62	13.53	16.07	14.04	12.38	6.66	8.92
Fe_2O_3	6.03	7.69	11.12	19.95	29.92	33.81	26.37
Na_2O	3.95	5.04	5.29	3.04	2.61	~0	~0
K_2O	4.60	5.86	8.48	10.08	7.31	42.04	64.76

All pyroxenes were calculated as aegirine, and all amphiboles – as arfvedsonite.

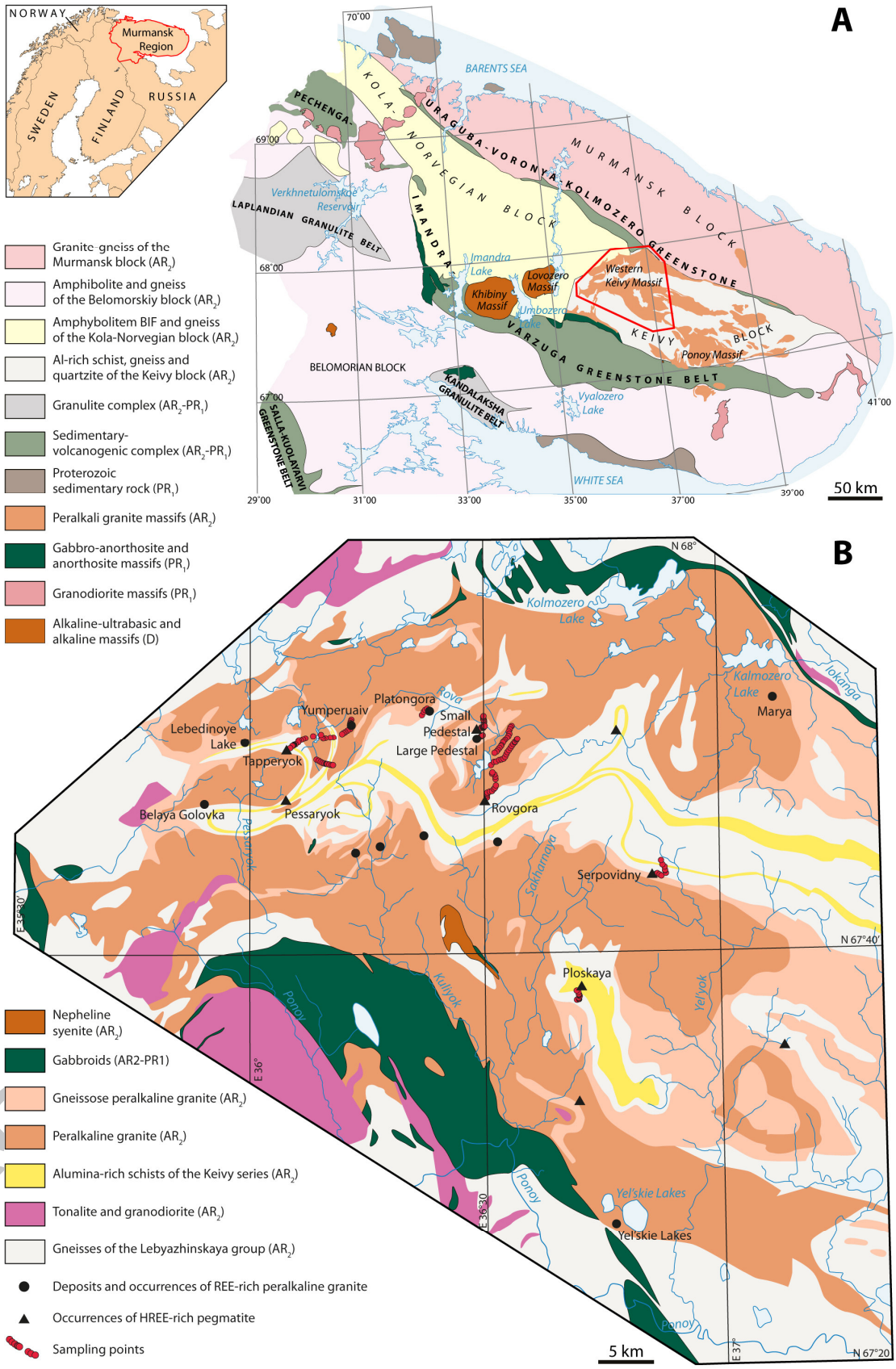

Fig. 1

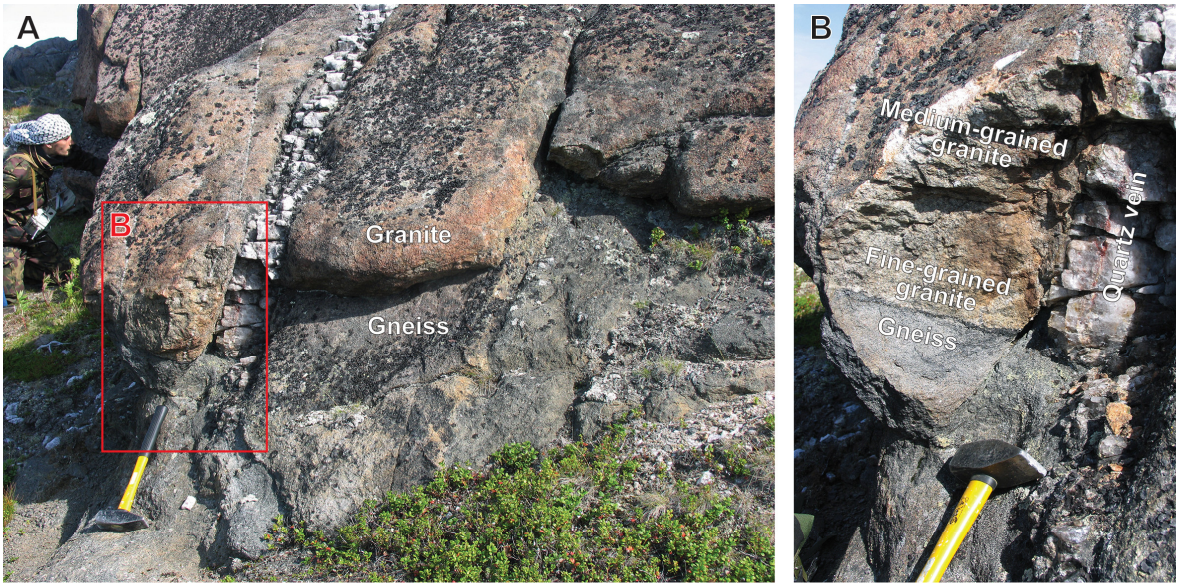

Fig. 2

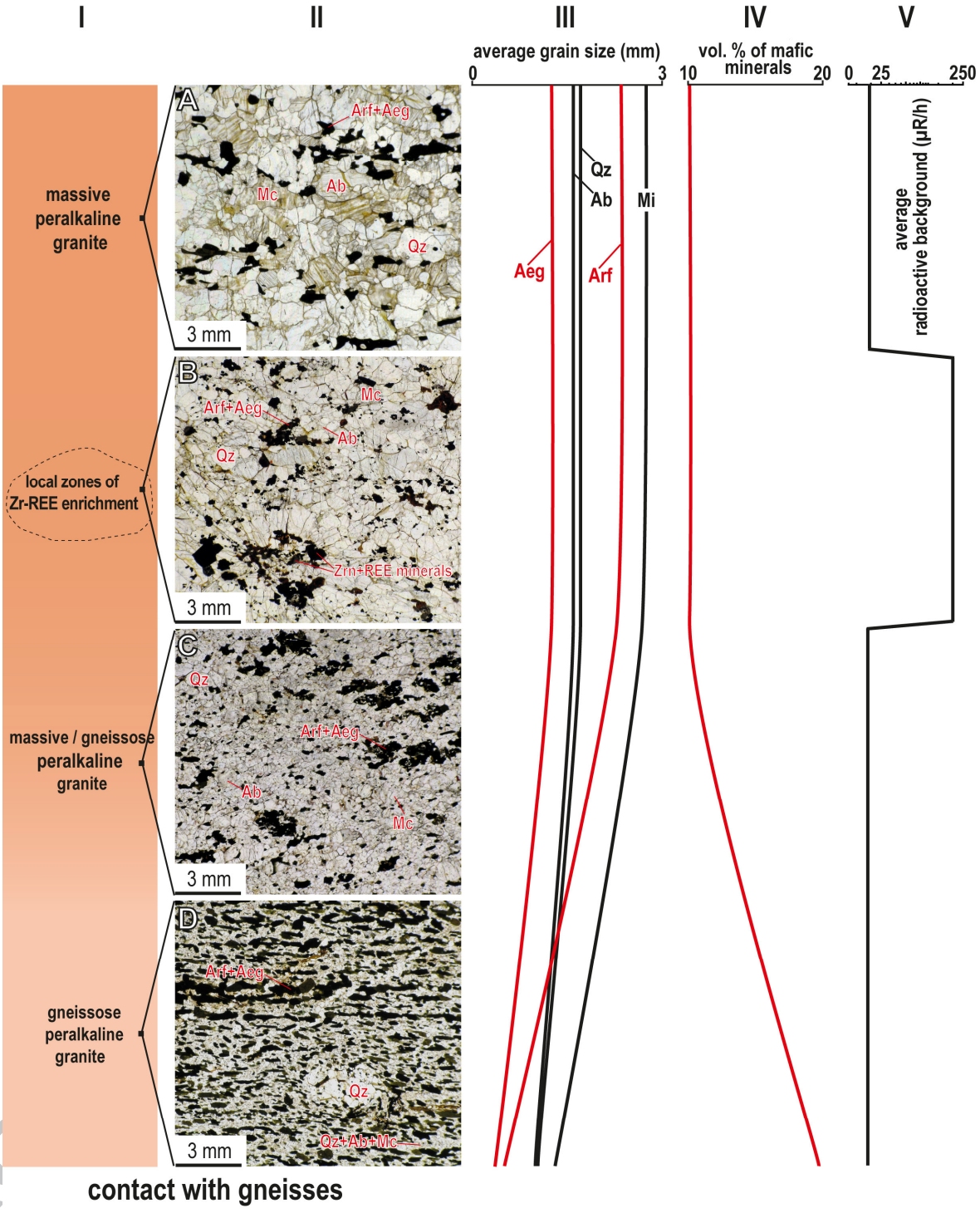
I
II
III
IV
V
average grain size (mm)
0
3
vol. % of mafic minerals
10
20
0
25
250
average radioactive background (µR/h)
massive peralkaline granite
local zones of Zr-REE enrichment
massive / gneissose peralkaline granite
gneissose peralkaline granite
A
Arf+Aeg
Mc
Ab
Qz
3 mm
B
Arf+Aeg
Mc
Ab
Qz
Zrn+REE minerals
3 mm
C
Qz
Arf+Aeg
Ab
Mc
3 mm
D
Arf+Aeg
Qz
Qz+Ab+Mc
3 mm
Qz
Ab
Mi
Aeg
Arf
contact with gneisses

Fig. 3

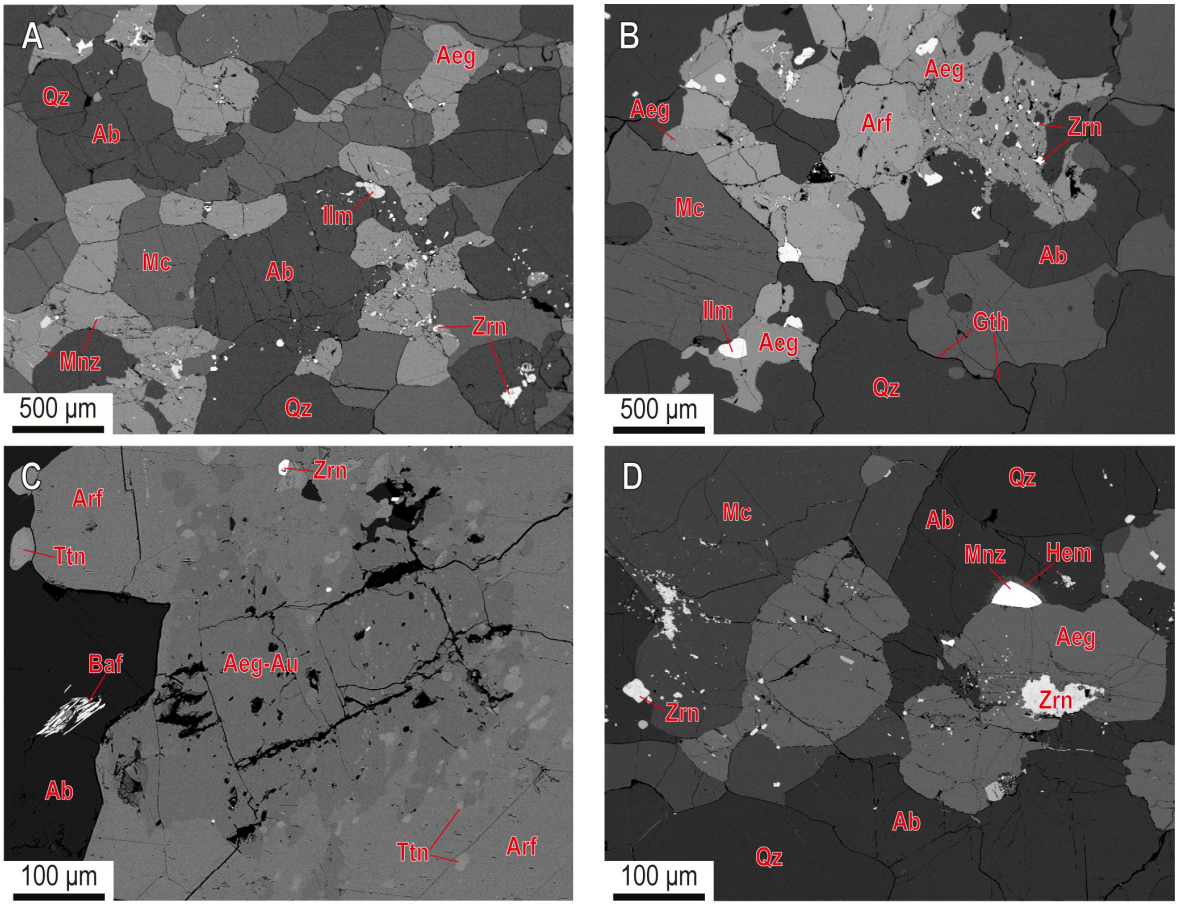

Fig. 4

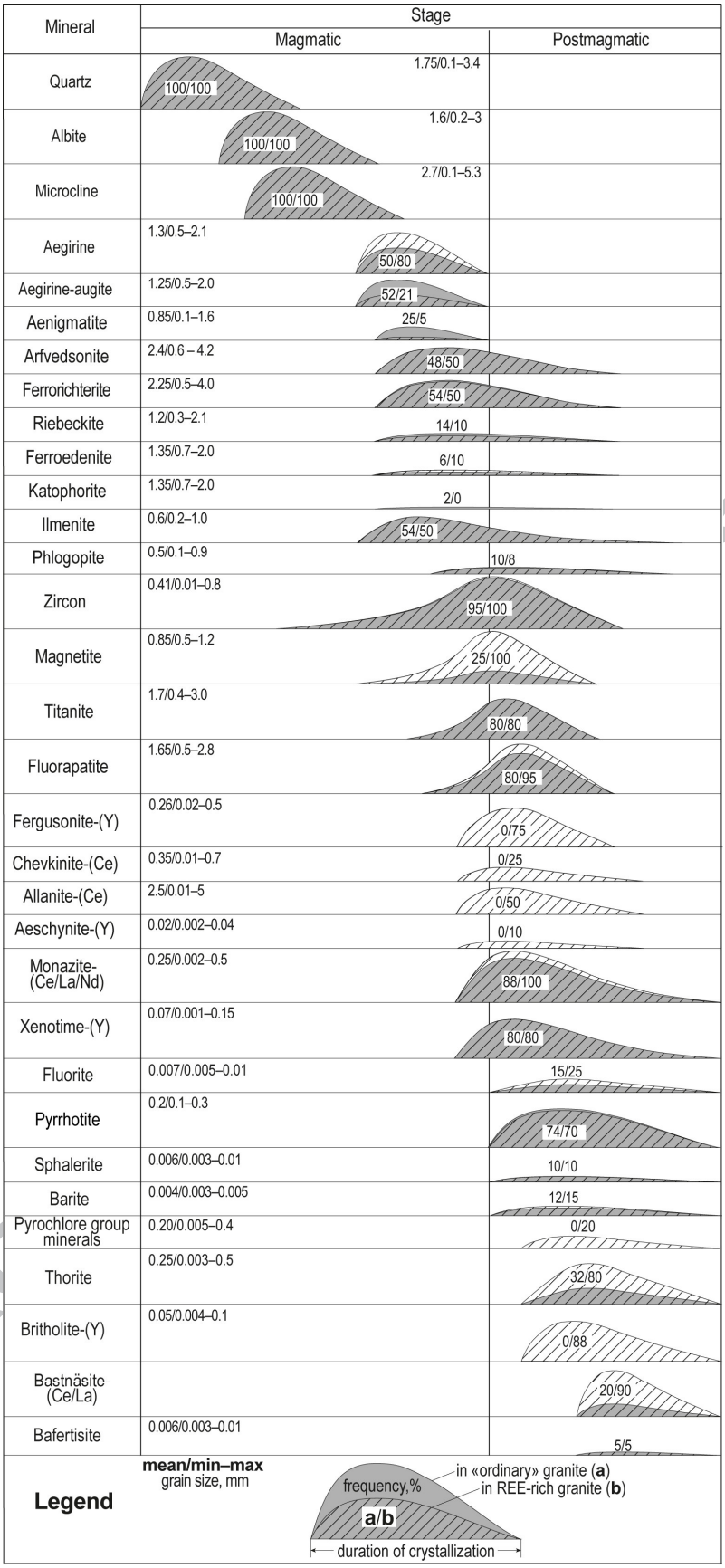

Fig. 5

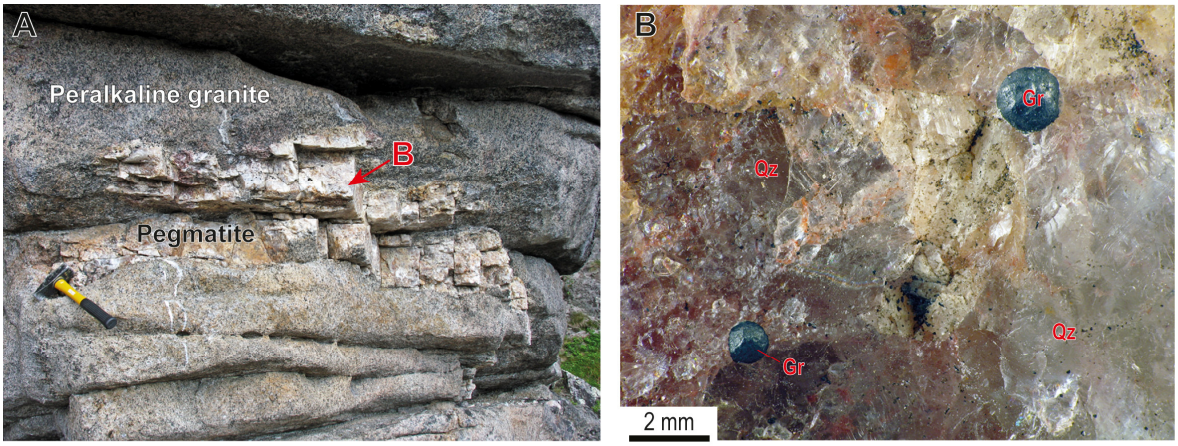

Fig. 6

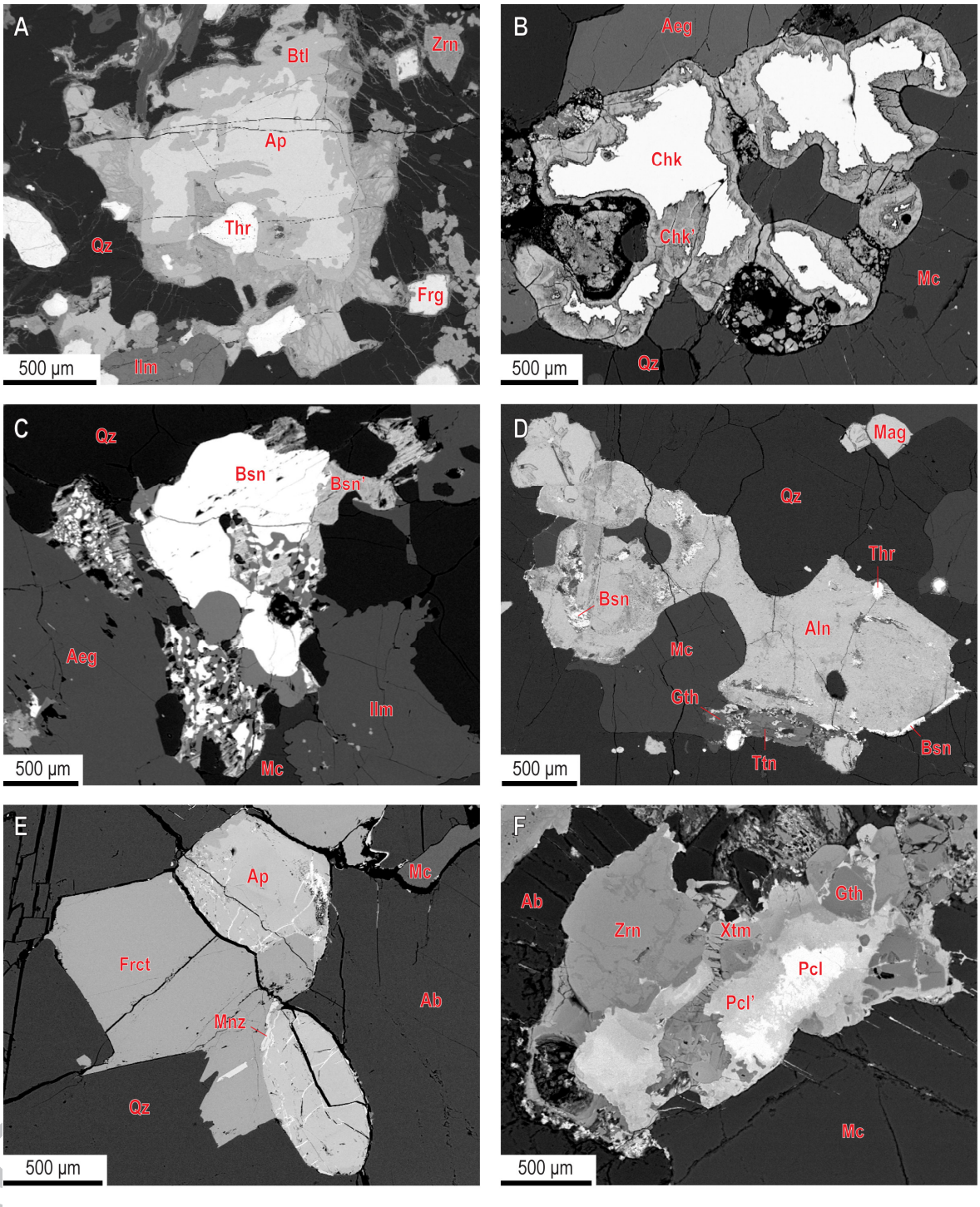
A
Btl
Zrn
Ap
Thr
Qz
Frg
500 µm
Ilm
B
Aeg
Chk
Chk'
Mc
500 µm
Qz
C
Qz
Bsn
Bsn'
Aeg
Ilm
500 µm
Mc
D
Mag
Qz
Thr
Bsn
Aln
Mc
Gth
Ttn
Bsn
500 µm
E
Ap
Mc
Frct
Ab
Mnz
Qz
500 µm
F
Ab
Gth
Zrn
Xtm
Pcl
Pcl'
Mc
500 µm

Fig. 7

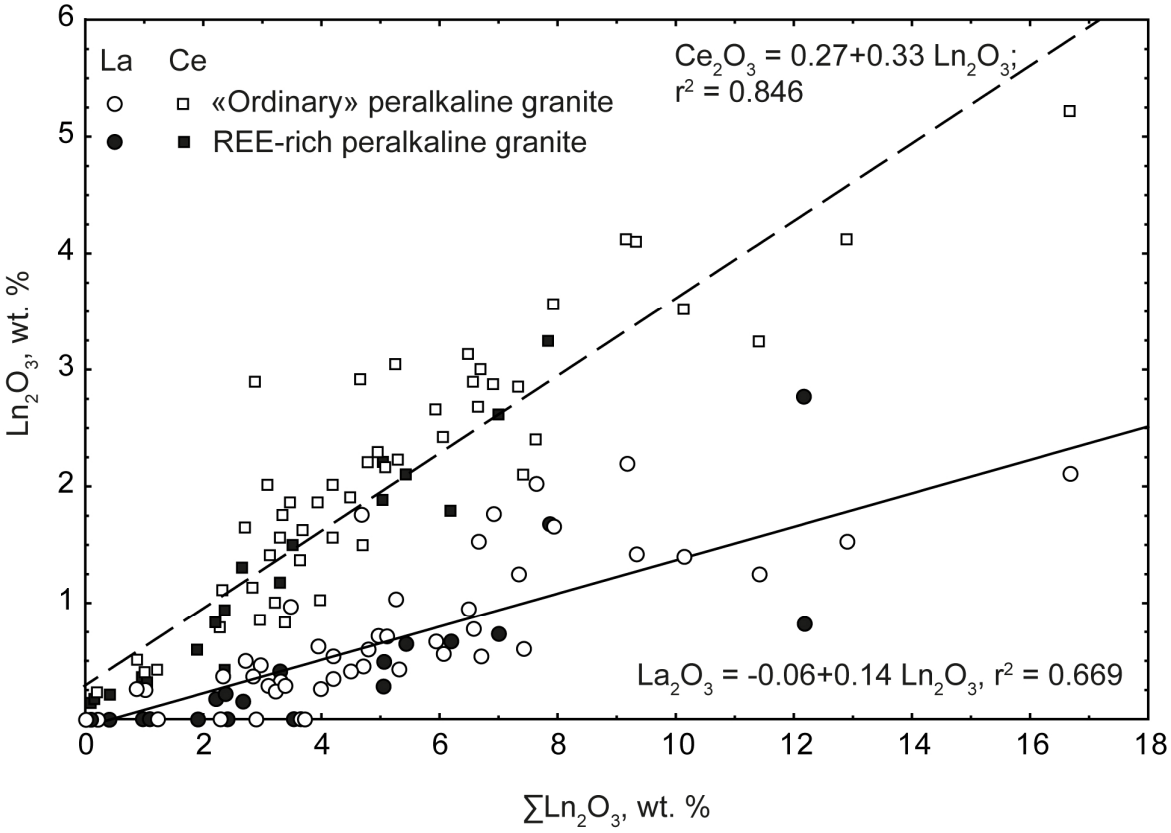

Fig. 8

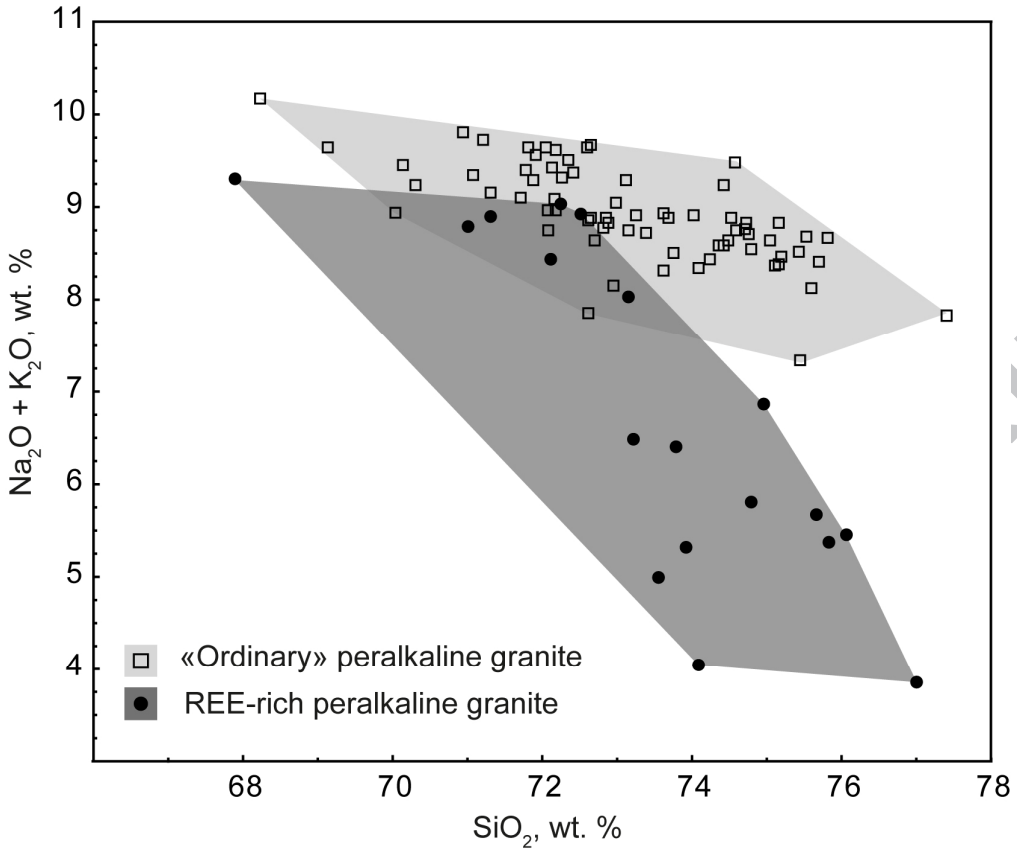

Fig. 9

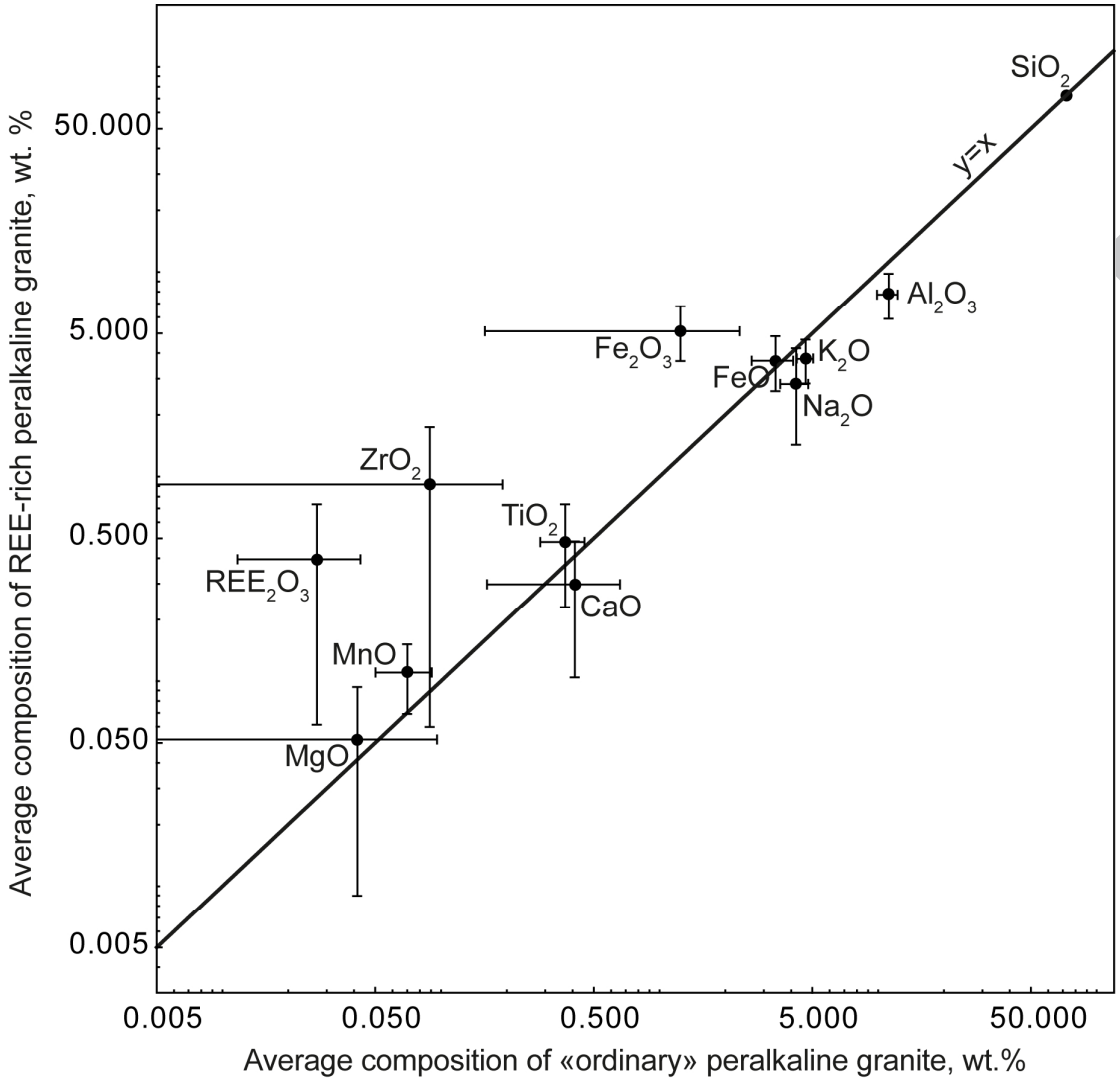
SiO2
y=x
Al2O3
Fe2O3
K2O
FeO
Na2O
ZrO2
TiO2
REE2O3
CaO
MnO
MgO
50.000
5.000
0.500
0.050
0.005
0.005
0.050
0.500
5.000
50.000
Average composition of REE-rich peralkaline granite, wt. %
Average composition of «ordinary» peralkaline granite, wt.%

Fig. 10

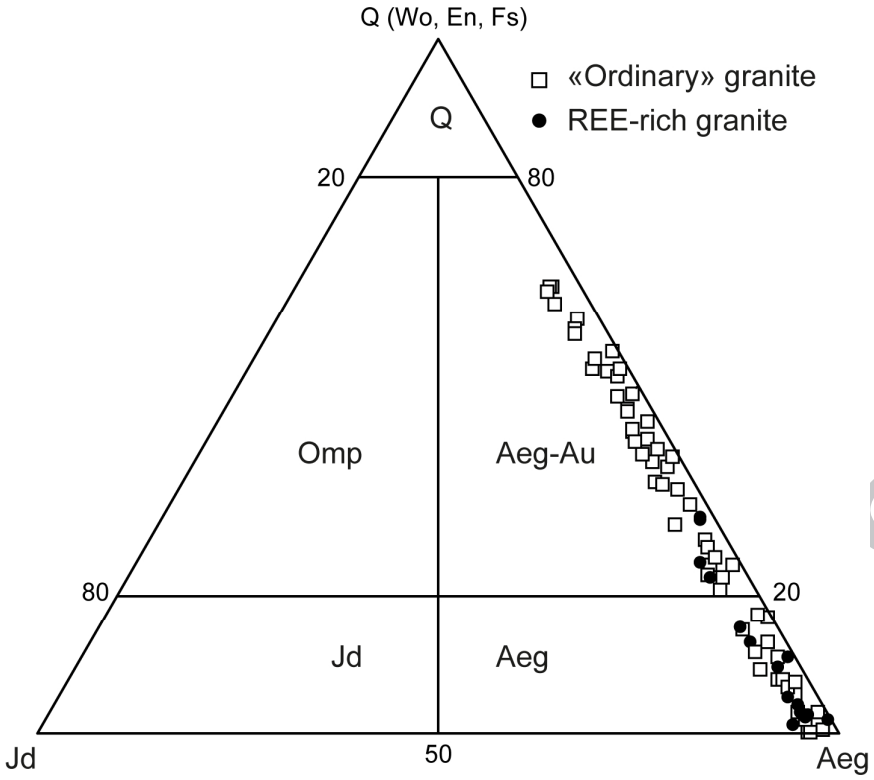

Fig. 11

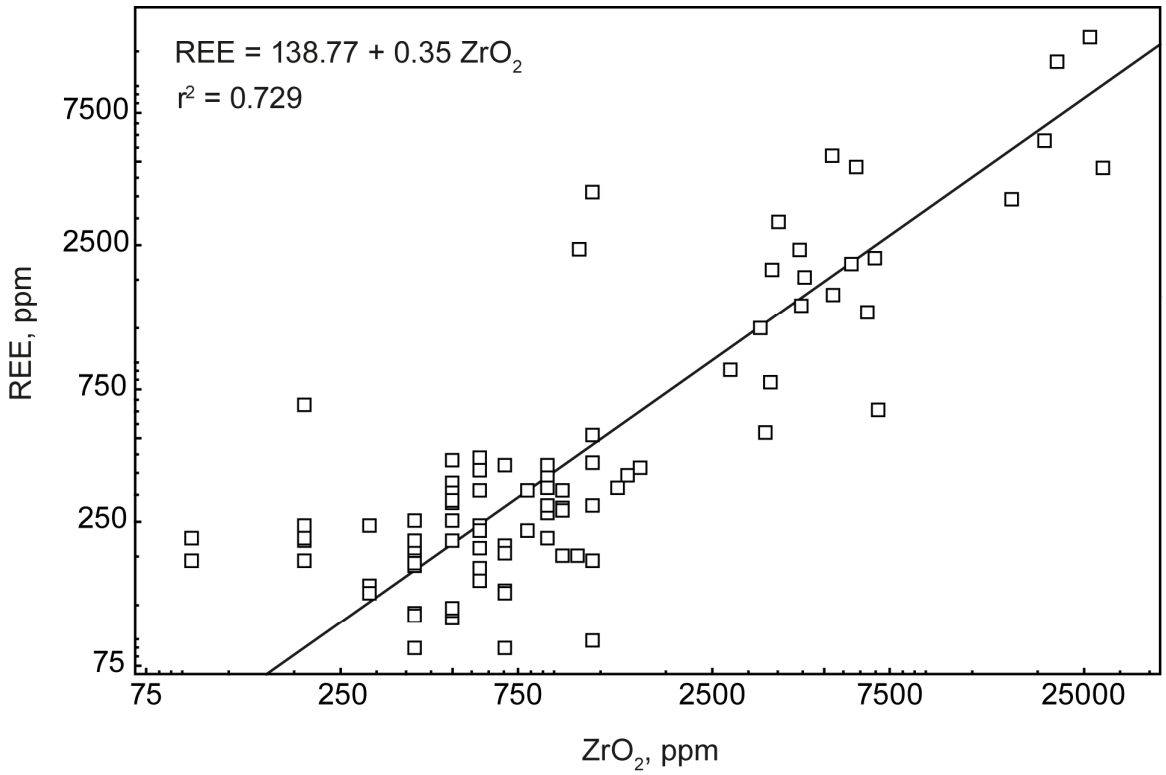

Fig. 12

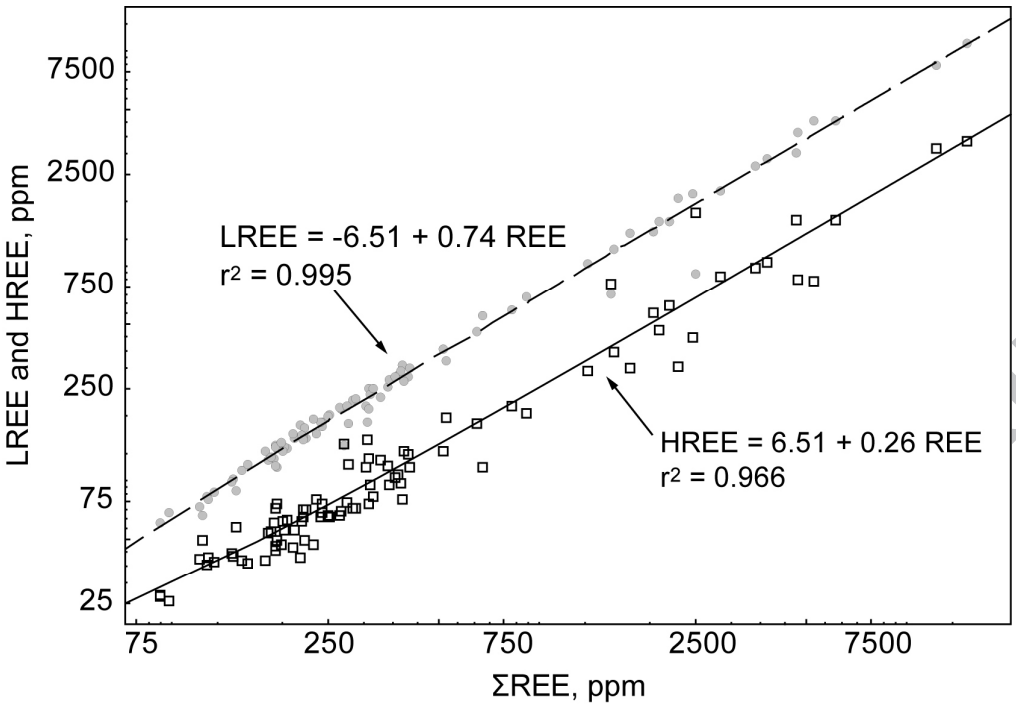

Fig. 13

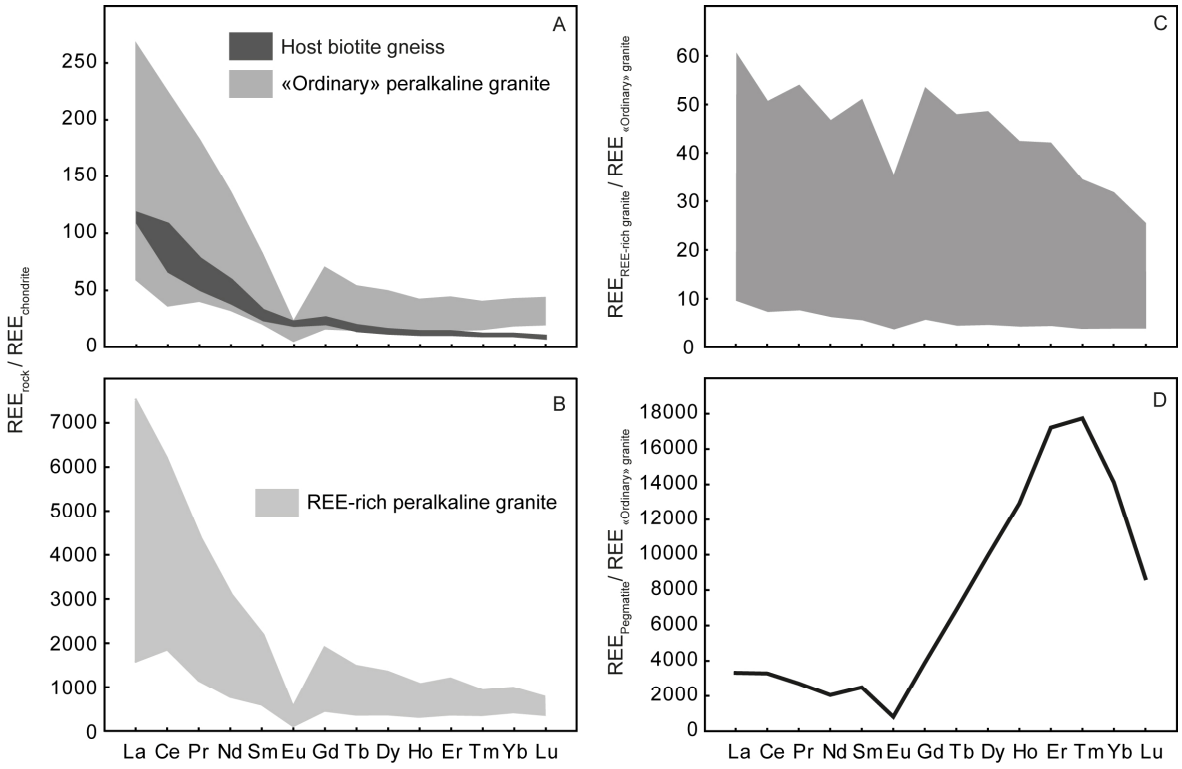

Fig. 14

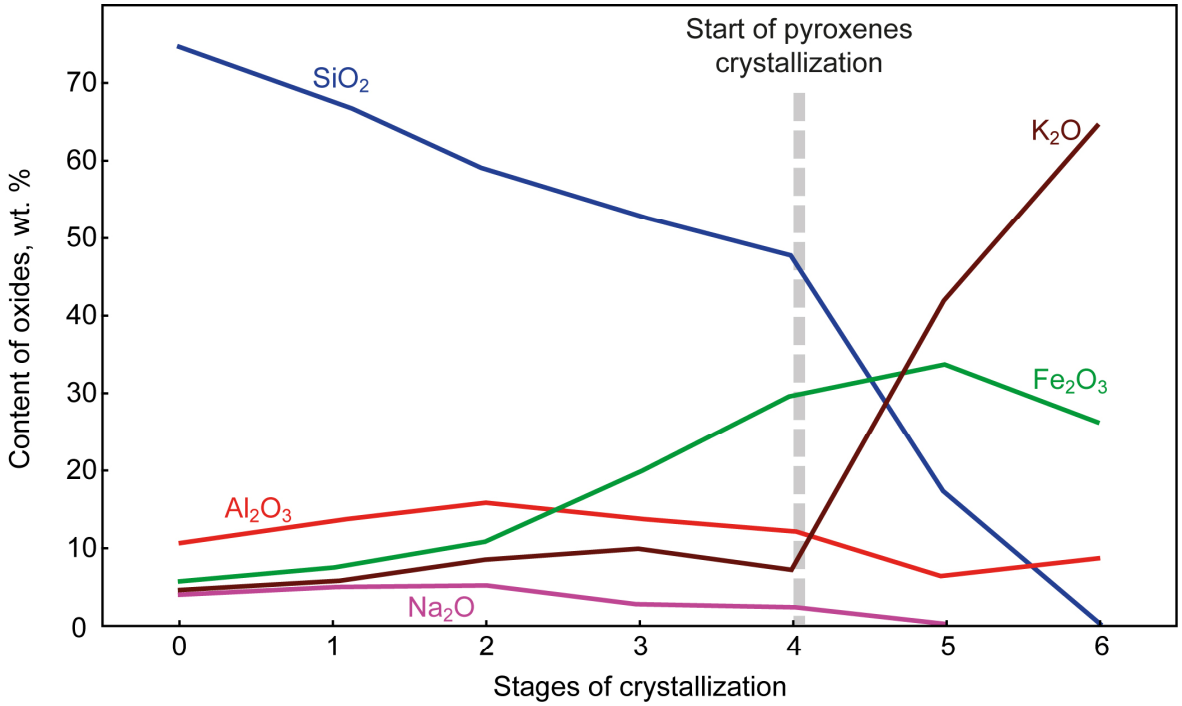

Fig. 15

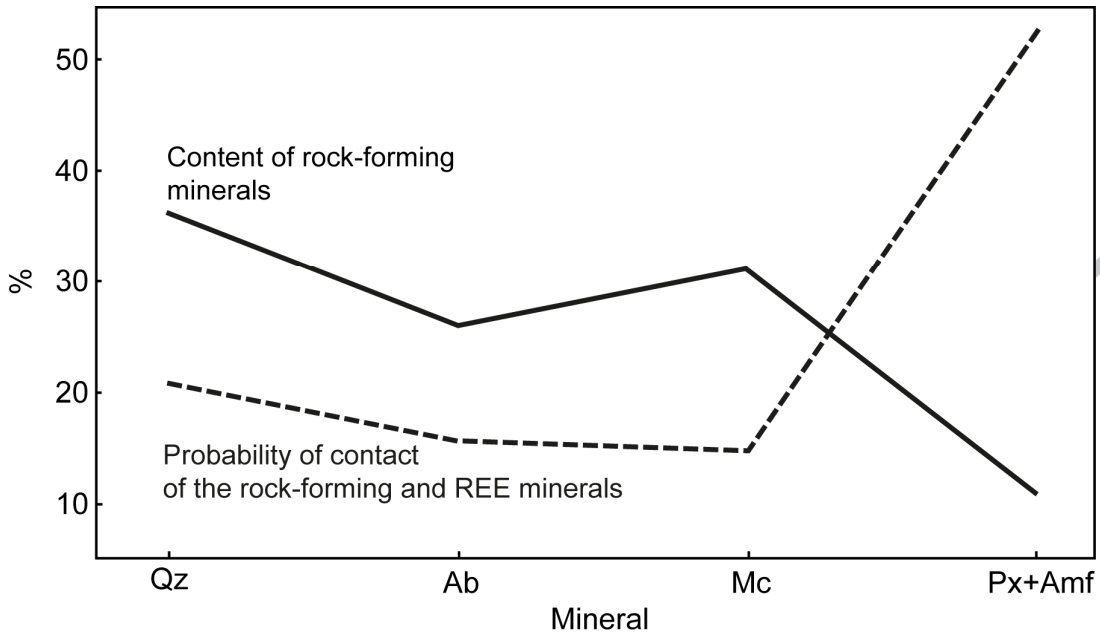

Fig. 16

Highlights

- The Western Keivy massif comprises the Yumperuaiv and Large Pedestal Zr-REE deposits
- The REE-rich granite originate from autometasomatical alteration of the peralkaline granite
- Chevkinite-(Ce), bastnäsite-(Ce) and fergusonite-(Y) are the main REE concentrators
- The granite massif generates HREE-rich quartz pegmatites